iScience

CellPress
OPEN ACCESS

Article

Elevated systemic total bile acids escalate susceptibility to alcohol-associated liver disease

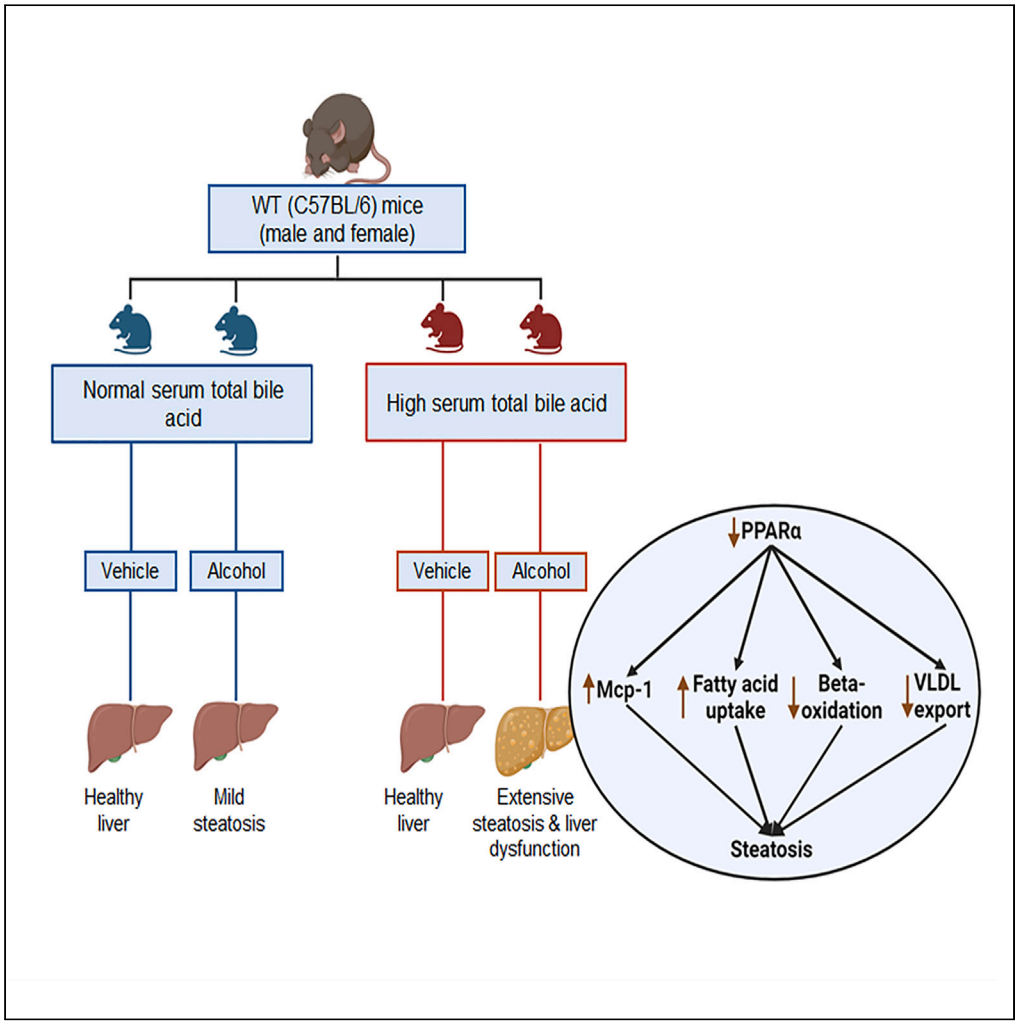

Devendra Paudel, Fuhua Hao, Umesh K. Goand, ..., Yuan Tian, Andrew D. Patterson, Vishal Singh

vxs28@psu.edu

Highlights

Cholemia (elevated serum TBA) exacerbated alcohol-associated liver disease (AALD)

Ethanol-fed cholemic mice exhibited increased susceptibility to hepatic steatosis

Reduced lipid metabolism gene expression linked to hepatic steatosis and dysfunction

Screening serum TBA could help identify individuals at high risk of developing AALD

Paudel et al., iScience 27, 110940
October 18, 2024
https://doi.org/10.1016/j.isci.2024.110940

iScience

CellPress
OPEN ACCESS

Article

Elevated systemic total bile acids escalate susceptibility to alcohol-associated liver disease

Devendra Paudel,[1] Fuhua Hao,[2] Umesh K. Goand,[1] Sangshan Tian,[1] Anthony M. Koehle III,[1] Loi V. Nguyen, Jr.,[1] Yuan Tian,[2] Andrew D. Patterson,[2] and Vishal Singh[1,3,4,5,*]

SUMMARY

Excessive alcohol consumption is a major global health problem. Individuals with alcoholic liver disease often exhibit elevated serum total bile acids (TBAs). Nevertheless, the extent to which high TBA contributes to alcohol-associated liver disease (AALD) remains elusive. To investigate this, wild-type mice were categorized into normal (nTBA) and high (hTBA) TBA groups. Both groups underwent chronic-binge ethanol feeding for 4 weeks, followed by additional weekly ethanol doses. Ethanol feeding worsened AALD in both male and female mice with elevated serum TBA, characterized by liver dysfunction and steatosis. Decreased hepatic expression of genes involved in mitochondrial β-oxidation and lipid transport in ethanol-fed hTBA mice suggests that altered fatty acid metabolism contributed to AALD. Our findings, which represent the first to link high serum TBA to increased AALD susceptibility, underscore the importance of proactive serum TBA screening as a valuable tool for identifying individuals at high risk of developing AALD.

INTRODUCTION

Excessive alcohol consumption currently ranks as the seventh leading cause of premature death and disability.[1] The National Institute on Alcohol Abuse and Alcoholism (NIAAA) defines binge drinking for men as consuming five or more drinks within 2 h, whereas for women, it is four or more drinks within the same time frame, potentially raising the blood alcohol concentration (BAC) to 0.08 gm/dL or higher.[2] Binge drinking is frequently observed among young individuals, wherein copious amounts of alcohol are consumed within a short time frame, often with the sole purpose of achieving a state of intoxication.[3] On average, approximately 21.5% of the US population—roughly 60 million individuals—engage in binge drinking each month.[4] Such excessive amounts of alcohol consumption significantly increase the risk of various health complications, including liver disease.

Cholemia is a condition characterized by high systemic total bile acids (TBAs). This condition arises due to changed physiological states, such as pregnancy (intrahepatic cholestasis of pregnancy [ICP]),[5] or due to congenital portosystemic shunts (CPSSs)[6,7] and specific liver diseases, including alcoholic and viral hepatitis.[8] Serum TBA level above 10 μM indicates ICP. Severe cases of ICP have bile acids above 40 μM[9] and pose a greater risk for pregnancy complications such as preterm labor and respiratory issues after birth.[10] In humans, CPSS[7] is caused by the presence of an obstructed blood vessel, resulting in diversion of portal flow to the systemic circulation.[11] Such an abnormal obstruction leads to an increased bile acid level in the bloodstream, giving rise to various symptoms such as lethargy, vomiting, and diarrhea, causing disruptions in metabolic and physiological processes.[12] Patients with portosystemic shunts (PSSs) frequently exhibit elevated bile acids in blood tests, and a subset of these individuals also show increased markers of liver dysfunction.[7] In severe cases, PSS can lead to the development of conditions such as hepatic encephalopathy, variceal bleeding, and portal vein thrombosis.[13] Current prevalence of PSS is not well established, as this condition can be congenital or acquired due to prior liver health issues[13] and can be asymptomatic as well.[14] However, few studies have reported the average incidence of congenital portosystemic shunt to be 1 in 30,000 to 50,000 live births.[15,16]

Elevated systemic TBA levels are frequently observed in patients with acute and chronic liver diseases.[17] Such an increase in serum bile acid, specifically during hepatitis, results from a malfunction of multiple hepatic mechanisms, including dysfunction of sinusoidal liver cell uptake, impaired transport within hepatocytes, and dysfunction of bile acid efflux at the bile duct domain.[18,19] Although patients with hepatitis exhibit elevated serum TBA levels, the extent to which this elevation contributes to liver disease remains unclear. To elucidate this, we studied the effects of elevated serum TBA on liver function in the presence or absence of chronic alcohol exposure using a mouse model. About 8%–15% of C57BL6/J strains of mice are born with PSS, making them valuable models to study the physiological implications of cholemia.[20] Similar to humans, the elevated serum TBA in these mice with PSS is due to obstructed liver vasculature, namely PSS. We categorized mice based on

[1]Department of Nutritional Sciences, The Pennsylvania State University, University Park, PA, USA
[2]Department of Veterinary and Biomedical Sciences, The Pennsylvania State University, University Park, PA, USA
[3]Center for Molecular Immunology and Infectious Disease, Huck Institutes of the Life Sciences, The Pennsylvania State University, University Park, PA, USA
[4]One Health Microbiome Center, Huck Institutes of the Life Sciences, The Pennsylvania State University, University Park, PA, USA
[5]Lead contact
*Correspondence: vxs28@psu.edu
https://doi.org/10.1016/j.isci.2024.110940

their pre-existing TBA: normal TBA (nTBA) and high TBA (hTBA). Liver function markers in the vehicle-treated groups (nTBA and hTBA) were comparable, suggesting that elevated serum TBA alone does not impact liver function. Notably, upon ethanol feeding, liver dysfunction markers substantially increased only in the hTBA group, not in the nTBA group. This observation suggests that pre-existing elevated TBA levels escalate susceptibility to alcohol-associated liver disease (AALD).

RESULTS

Ethanol consumption induces liver injury and hepatic steatosis in both male and female mice with cholemia

Elevated serum TBA regulating the AALD progression remains largely unexplored. Therefore, to determine the impact of high systemic TBA on AALD progression, 12-week-old, both male and female wild-type (WT) mice with normal TBA (nTBA, average: 9.87 μM; confidence interval [CI] [95%]: 8.92–10.82) and high TBA (hTBA, average: 102.02 μM; CI [95%]: 88.96–115.07) (Figure 1A) were maintained on a standard chow diet and fed either water (vehicle) or ethanol (20%, v/v, Alc) *ad libitum*. After 1 week, the ethanol-fed group also received four weekly ethanol (3.2 g/kg b. wt.) oral gavage (Figure 1B). High TBA mice fed ethanol (hTBA+Alc) exhibited greater body weight loss compared to the hTBA+Veh group and the normal TBA groups (nTBA+Veh and nTBA+Alc) (Figure 1C). Notably, the biomarkers of liver dysfunction alanine transaminase (ALT) and aspartate transaminase (AST) were significantly elevated in hTBA+Alc compared to the other groups (hTBA+Veh, nTBA+Veh, and nTBA+Alc) (Figures 1D and 1E). The histological analysis revealed hepatic micro-steatosis in hTBA+Alc group (Figure 1F). Mice in the high TBA ethanol group (hTBA+Alc) had significantly higher levels of alkaline phosphatase (ALKP) compared to the other groups (Figure 1G). However, albumin (ALB) and total bilirubin (TBIL) levels were comparable across all groups (Figures 1H and 1I). Research studies have revealed sex-specific differences in alcohol-induced liver disease.[21,22] We employed the similar ethanol intervention regime in female WT (C57BL/6) mice. The female mice cohort displayed similar findings: the hTBA group exhibited hepatic steatosis and liver dysfunction upon ethanol feeding (Figures 2A–2I). To determine whether elevated serum TBA independently affects liver function, we measured liver function markers (ALT and AST) prior to any intervention in mice with normal TBA and high TBA. Intriguingly, high TBA mice exhibited reduced levels of ALT and AST prior to ethanol intervention (Figures S1A and S1B), indicating that elevated TBA alone is not sufficient to cause liver dysfunction in mice. However, upon ethanol feeding, both male and female mice with high TBA displayed hepatic lipid accumulation and liver dysfunction. Collectively, our results demonstrate that pre-existing cholemia (elevated serum TBA) predisposes mice to AALD.

Patients with alcoholic hepatitis display elevated serum TBA levels.[23] Therefore, we evaluated the serum TBA in both male and female mice and found that alcohol feeding increased bile acid levels specifically in mice with cholemia (Figures S2A and S2B), suggesting that alcohol-induced liver injury in cholemic mice further potentiated systemic accumulation of TBA in mice with pre-existing cholemia.

To further confirm our findings, we used Lieber-DeCarli liquid diet model, developed by the National Institute on Alcohol Abuse and Alcoholism (NIAAA),[24] which is considered as a gold-standard model in studying the effect of alcohol consumption on liver dysfunction. This model is based on liquid diet feeding where ethanol is mixed with liquid diet, forcing the mice to consume ethanol while eating diet. As a result, these mice display a strong disease phenotype. Notably, in agreement with the long-term ethanol feeding model, the high TBA group maintained on ethanol-supplemented Lieber-DeCarli liquid diet exhibited extensive liver injury and lipid accumulation (Figures S3A–S3H). This observation in the Lieber-DeCarli liquid diet model further strengthens our finding that cholemia predisposes mice to AALD.

Ethanol feeding exacerbates hepatic lipid accumulation in mice with pre-existing cholemia

Disruptions in lipid metabolism play a pivotal role in the pathogenesis of alcohol-related steatotic liver disease, as alcohol stands out among the toxins capable of inducing disturbances across various lipid metabolic processes in the liver.[25] This, in turn, leads to heightened hepatic fatty acid uptake, decreased β-oxidation, and increased synthesis of triglycerides via *de novo* lipogenesis. Next, we investigated the hepatic lipid profile in both male and female mice cohort using 1H NMR spectroscopy to assess the extent of lipid accumulation in response to ethanol intervention. We observed significantly higher levels of triglycerides, total cholesterol, saturated fatty acids, unsaturated fatty acids, and total fatty acids in hTBA+Alc, compared to the other groups (Figures 3A–3E), suggesting that pre-existing cholemia potentiated ethanol-induced hepatic steatosis. Of note, the ethanol groups exhibited heightened levels of unsaturated fatty acids, including monounsaturated fatty acid (MUFA), polyunsaturated fatty acids (PUFAs) such as ω-3 fatty acid, docosahexaenoic acid (DHA), and linoleic acid (LA)—commonly recognized as beneficial or healthy fats (Figures 3F–3I). Phosphatidylcholine, a type of phospholipid widely used to treat steatotic liver disease,[26] was significantly decreased in ethanol-fed mice with high TBA compared to other groups (Figure 3J). We did not observe differences in total polyunsaturated fatty acid (PUFA), arachidonic and eicosapentaenoic acid (ARA and EPA), and other lipids in the liver such as free cholesterol (FC), cholesterol ester (CE), phosphatidylethanolamine (PE), and sphingomyelin (Figure 3K). Ethanol-fed hTBA female group, like male, exhibited elevated levels of triglycerides, total cholesterol, and fatty acids (Figures 4A–4I). Female mice also had reduced phosphatidylcholine (Figure 4J). Consistent with the male mice, the female hTBA+Alc group also showed no significant changes in PUFA, ARA and EPA, FC, CE, PE, and sphingomyelin levels (Figure 4K). Notably, the female nTBA+ Alc group displayed significant elevation of hepatic triglycerides, saturated fatty acids, unsaturated fatty acids, and total fatty acids compared to respective control (nTBA+ veh) (Figures 4A–4D). Although these lipid species showed an upward trend in male nTBA+Alc group, these changes were not statistically significant (Figures 3A–3D). Collectively, ethanol consumption in cholemic mice led to a distinct accumulation of lipid species that are linked to promote AALD progression, suggesting that pre-existing cholemia significantly amplified ethanol's detrimental effects on liver fat metabolism and potentially accelerated AALD development.

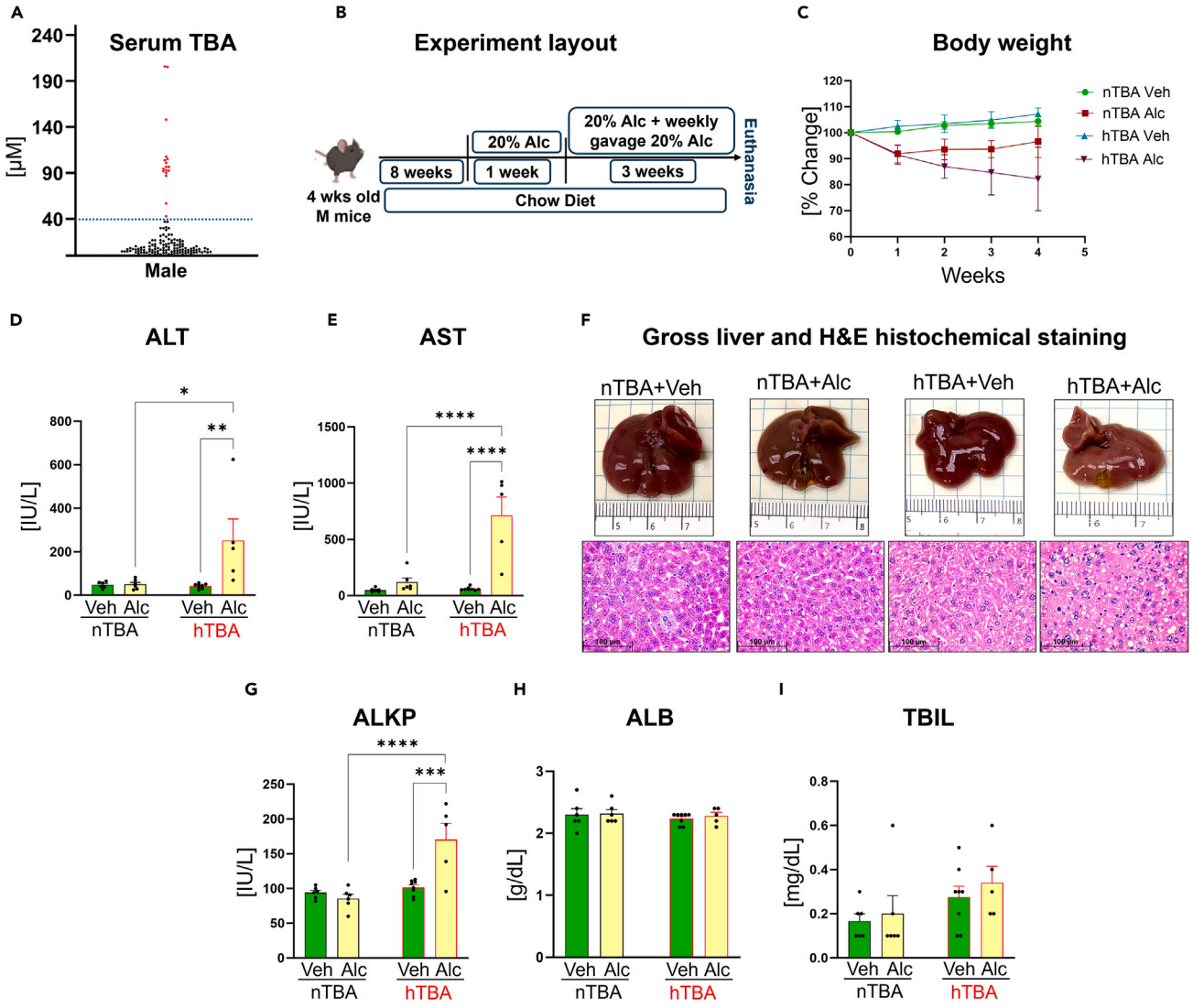

Figure 1. Ethanol feeding increases susceptibility to hepatic steatosis in male mice with cholemia

(A) Screening of male mice for TBA levels (each dot represents one mouse; *n* = 134).

(B) Experimental layout for ethanol intervention.

(C) Percent change in body weight. Serum levels of (D) ALT and (E) AST.

(F) Gross liver and representative H&E images of liver [original magnification, x200].

(G–I) Serum levels of ALKP, ALB, and TBIL. (ALT, alanine aminotransferase; AST, aspartate aminotransferase; ALKP, alkaline phosphatase; ALB, albumin; TBIL, total bilirubin). Data are represented as mean ± SEM (*n* = 5–7 mice/group, **p* < 0.05, ***p* < 0.01, ****p* < 0.001, *****p* < 0.0001 by ANOVA with Tukey's post hoc test).

Ethanol consumption induces *Mcp1* and alters the expression of genes related to liver lipid metabolism in cholemic mice

The level of monocyte chemoattractant protein-1 (MCP1), a chemokine involved in immune cell recruitment, is elevated in patients with AALD, and the mice lack *Mcp1* gene exhibit protection against alcohol-induced liver injury.[27] As a potent inducer of monocyte recruitment and activation, *Mcp1* is primarily regulated at the transcriptional level and can be triggered by factors such as lipopolysaccharides, tumor necrosis factor alpha (TNF-α), and interleukin-1 (IL-1).[28] Previous studies have linked *Mcp1* to hepatic lipid dysregulation.[29,30] Therefore, we estimated the mRNA transcripts of hepatic *Mcp1* and genes involved in lipid metabolism using quantitative RT-PCR. Our analysis showed a substantial upregulation in the hepatic *Mcp1*, particularly in hTBA+Alc group (Figure 5A). Concurrently, a distinctive reduction of peroxisome proliferator-activated receptor alpha (*Pparα*), a transcriptional regulator of genes associated with lipid metabolism, was observed in the hTBA+Alc group compared to other groups (Figure 5B). The hepatic expression of farnesoid X receptor (*Fxr*), a bile acid receptor, remained unaltered (Figure 5C). Moreover, a higher expression of *Cd36*, a scavenger receptor involved in hepatic fatty acid uptake, was observed in ethanol-fed hTBA group (Figure 5D). Expression of genes implicated in mitochondrial β-oxidation, namely sirtuin-1 (*Sirt1*) and carnitine

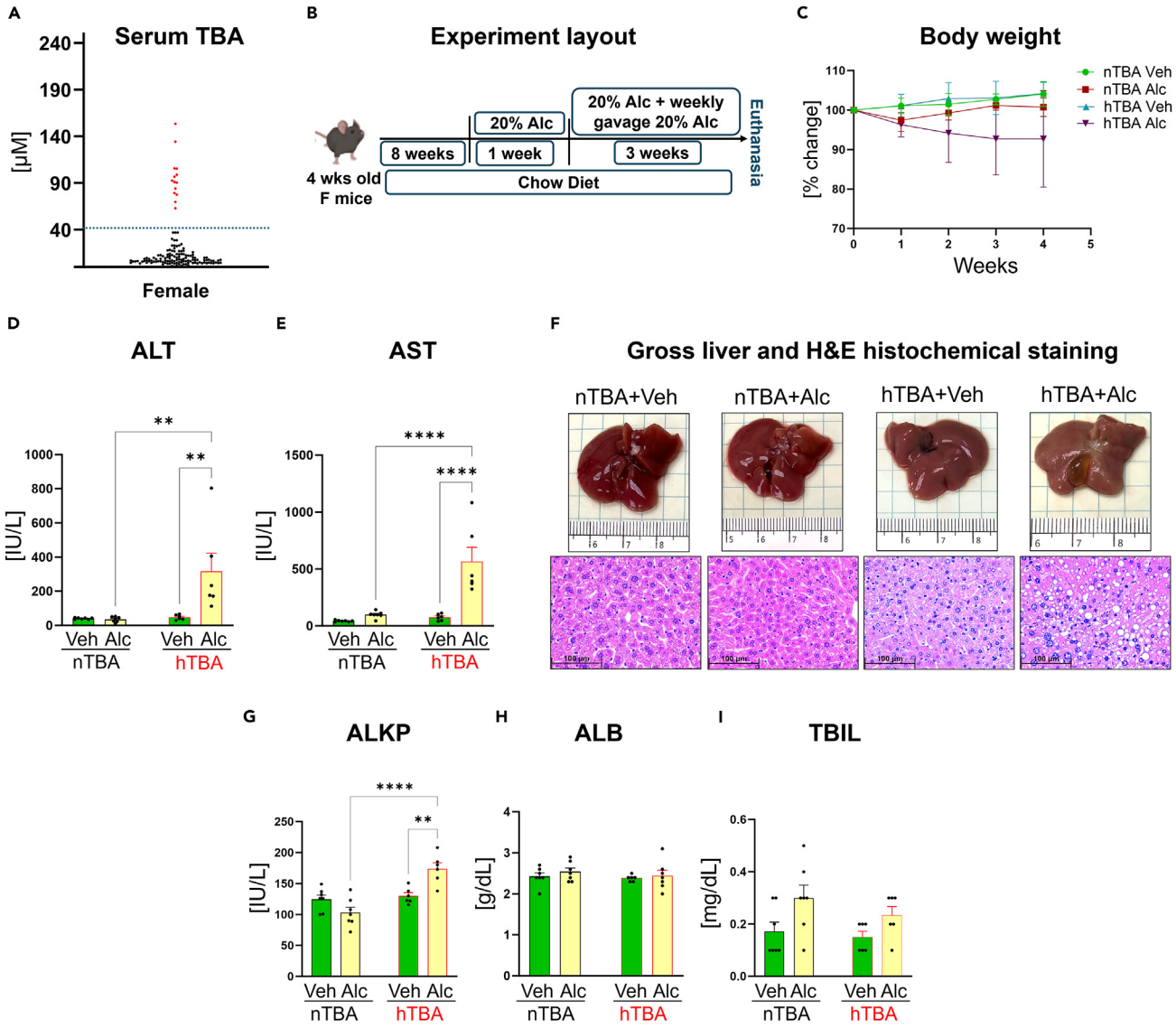

Figure 2. Female mice with pre-existing cholemia displayed ethanol-induced hepatic dysfunction

(A) Screening of female mice for TBA levels (each dot represents one mouse; $n = 138$).

(B) Experimental outline for ethanol intervention.

(C) Percent change in body weight. Serum levels of (D) ALT and (E) AST.

(F) Gross liver and representative H&E images of liver (original magnification, x200).

(G–I) Serum levels of ALKP, ALB, and TBIL. (ALT, Alanine aminotransferase; AST, aspartate aminotransferase; ALKP, alkaline phosphatase; ALB, albumin; TBIL, total bilirubin). Data are represented as mean ± SEM ($n = 5$–7 mice/group, *$p < 0.05$, **$p < 0.01$, ***$p < 0.001$, ****$p < 0.0001$ by ANOVA with Tukey's post hoc test).

palmitoyltransferase 1 (*Cpt1*), was substantially decreased in the hTBA group (Figures 5E and 5F). Furthermore, the ethanol-fed hTBA mice exhibited decreased hepatic expression of genes related to hepatic fatty acid transport, including microsomal triglyceride transfer protein (*Mtp*) and apolipoprotein B (*Apob*) (Figures 5G and 5H). Surprisingly, hTBA group showed reduced expression of lipogenic gene stearoyl-CoA desaturase 1 (*Scd1*), whereas ethanol-fed mice with normal bile acid (nTBA group) displayed increased *Scd1* (Figure 5I). Similarly, fatty acid synthase (*Fas*), another crucial lipogenic gene, also showed a decreased expression in the ethanol-fed hTBA group (Figure 5J). The expression of sterol regulatory element-binding protein-1c (*Srebp1c*), a transcription factor that regulates lipogenesis in the liver, remained unaltered in all groups (Figure 5K). We further confirmed the expression of these markers in the female mice cohort. Interestingly, mirroring the findings in males, ethanol-fed female hTBA+Alc group also exhibited increased hepatic expression of *Mcp1* and *Cd36* (Figures 6A and 6D). Likewise, the levels of *Pparα*, *Sirt1*, *Mtp*, and *Apob* were decreased (Figures 6B–6E, 6G, and 6H). No significant change was observed in *Fxr* (Figure 6C), although a decreasing trend was noted for *Cpt1* (Figure 6F). Notably, female hTBA+Alc group displayed increased expression

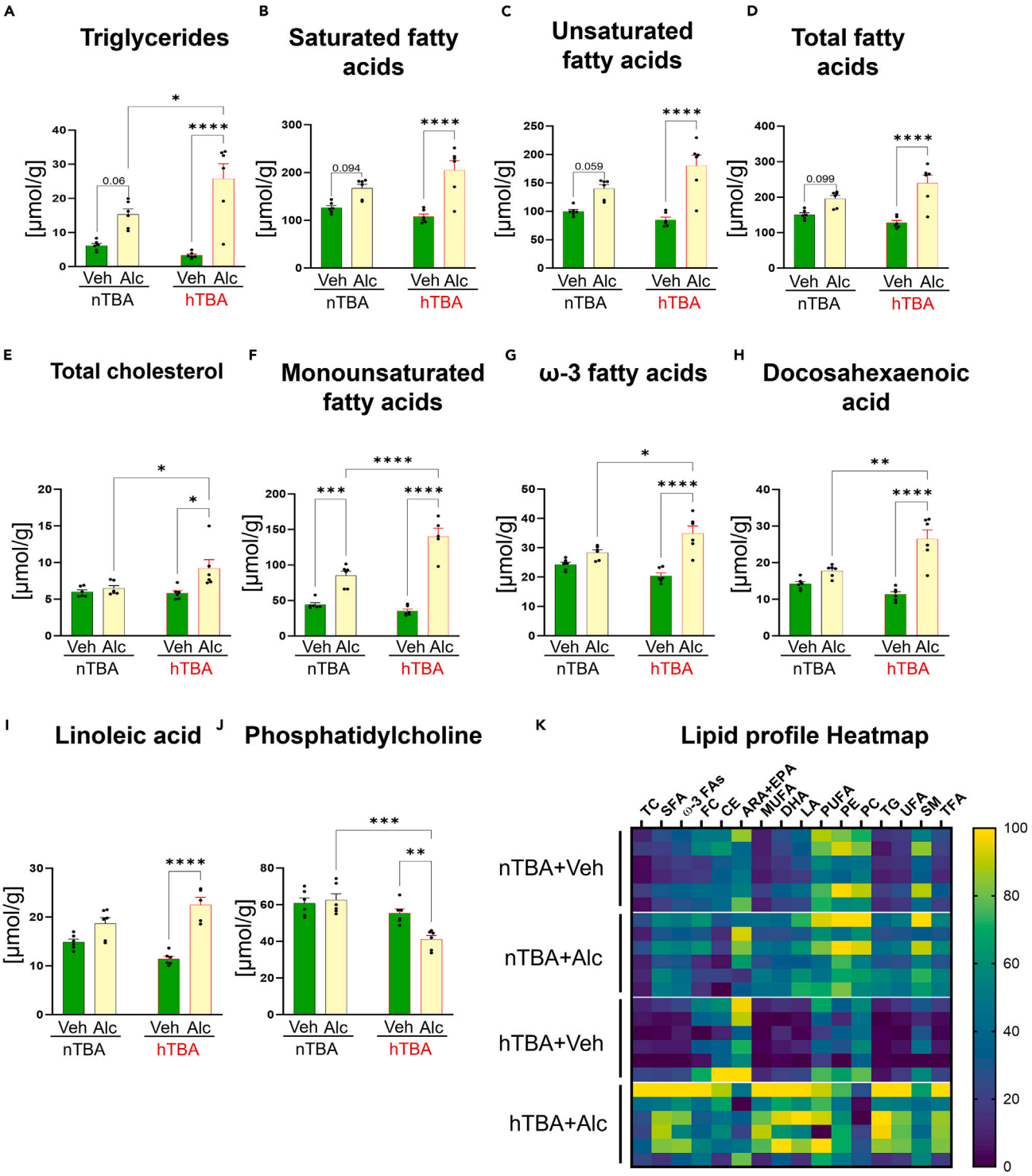

Figure 3. Cholemia aggravates liver lipid accumulation in male mice following chronic ethanol feeding

Hepatic levels of (A) triglycerides, (B) saturated fatty acids, (C) unsaturated fatty acids, (D) total fatty acids, (E) total cholesterol, (F) monounsaturated fatty acids, (G) ω-3 fatty acid, (H) docosahexaenoic acid, (I) linoleic acid, and (J) phosphatidylcholine.

(K) Heatmap showing lipid profile. (TC, total cholesterol; SFA, saturated fatty acid; ω-3 FA, omega-3 fatty acid; FC, free cholesterol; CE, cholesterol ester; ARA+EPA, arachidonic + eicosapentaenoic acid; MUFA, monounsaturated fatty acid; DHA, docosahexaenoic acid; LA, linoleic acid; PUFA, polyunsaturated fatty acid; PE, phosphatidylethanolamine; PC, phosphatidylcholine; TG, triglycerides; UFA, unsaturated fatty acid; SM, sphingomyelin; TFA, total fatty acid). Data are represented as mean ± SEM (n = 6 mice/group, *p < 0.05, **p < 0.01, ***p < 0.001, ****p < 0.0001 by ANOVA with Tukey's post hoc test).

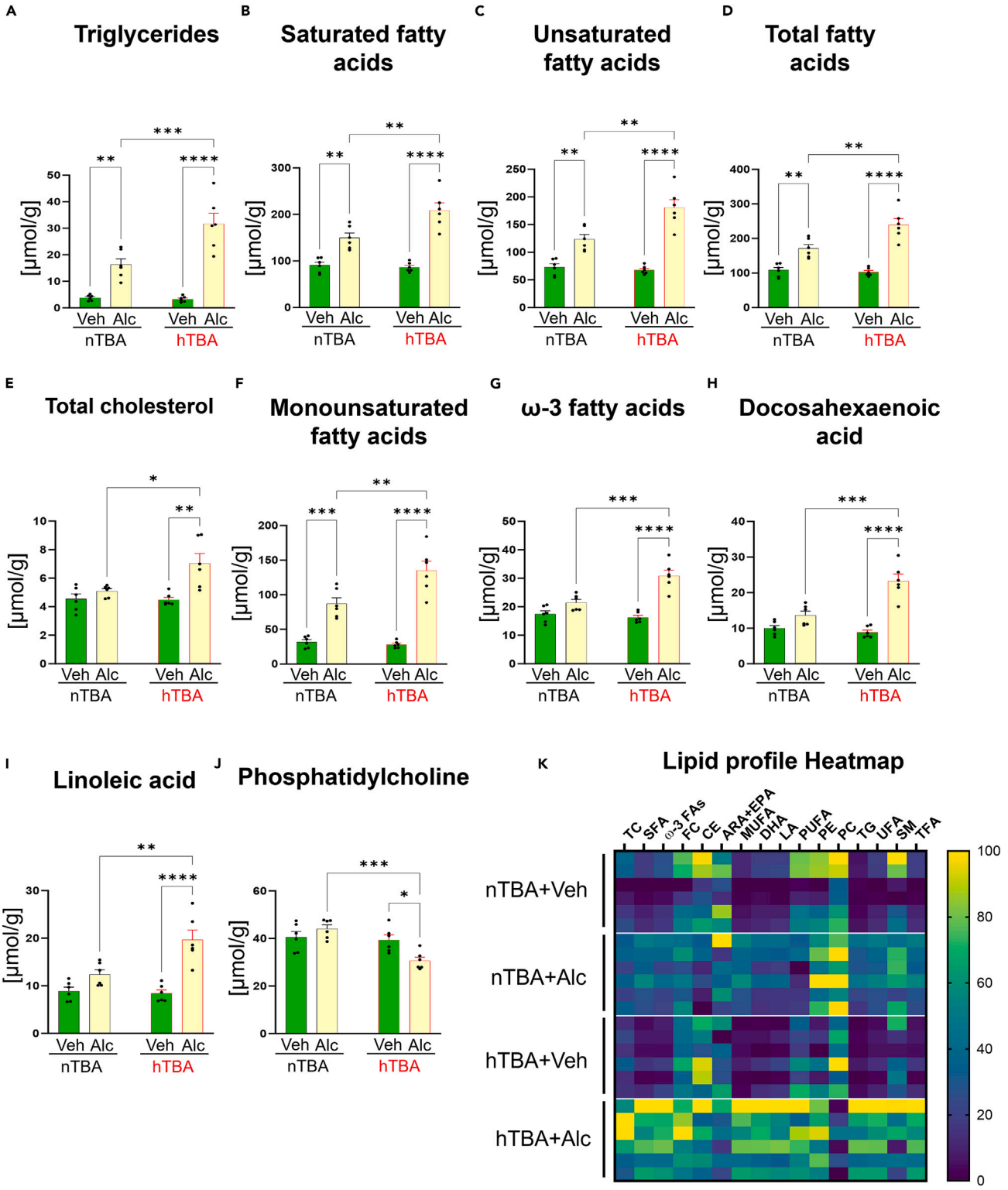

Figure 4. Chronic ethanol feeding promotes hepatic lipid accumulation in female mice with elevated TBA

Hepatic levels of (A) triglycerides, (B) saturated fatty acid, (C) unsaturated fatty acid, (D) total fatty acids, (E) total cholesterol, (F) monounsaturated fatty acid, (G) ω-3 fatty acid, (H) docosahexaenoic acid, (I) linoleic acid, and (J) phosphatidylcholine.

Figure 4. *Continued*

(K) Heatmap showing lipid profile. (TC, total cholesterol; SFA, saturated fatty acid; ω-3 FA, omega-3 fatty acid; FC, free cholesterol; CE, cholesterol ester; ARA+EPA, arachidonic + eicosapentaenoic acid; MUFA, monounsaturated fatty acid; DHA, docosahexaenoic acid; LA, linoleic acid; PUFA, polyunsaturated fatty acid; PE, phosphatidylethanolamine; PC, phosphatidylcholine; TG, triglycerides; UFA, unsaturated fatty acid; SM, sphingomyelin; TFA, total fatty acid). Data are represented as mean ± SEM (n = 6 mice/group, *p < 0.05, **p < 0.01, ***p < 0.001, ****p < 0.0001 by ANOVA with Tukey's post hoc test).

of hepatic *Srebp1c* compared to nTBA+Alc (Figure 6K). In the nTBA+Alc group, hepatic expression of *Scd1* and *Fas* was increased. However, the female hTBA+Alc group did not show any changes in hepatic *Scd1* or *Fas* levels compared to their respective controls (Figures 6I and 6J).

To gain mechanistic insight into how ethanol feeding induces hepatic injury and lipid accumulation in the mice with elevated TBA, we examined the extent of necrosis/apoptosis and inflammation via terminal deoxynucleotidyl transferase dUTP nick-end labeling (TUNEL) assay and ELISA (Table 1), respectively. Surprisingly, we did not observe any significant difference in TUNEL-positive cells between ethanol- and vehicle-treated normal or high TBA groups (Figure S4), suggesting that necrosis/apoptosis may not be a primary driver of injury in these groups. Although elevated *Mcp1* mRNA expression (Figure 5A) suggests immune cell infiltration, we did not observe elevated levels of inflammatory cytokines TNF-α and IL-1β in ethanol-fed groups (Figures S5A and S5B), indicating that hepatic inflammation is likely not occurring. Interestingly, the hepatic level of lipocalin 2 (Lcn2), an acute-phase protein previously shown to have a detrimental role in AALD,[31] was significantly increased in the ethanol-fed high-TBA group (Figure S5C). Altogether, these data suggest that a 4-week ethanol feeding regimen primarily induces steatosis without significantly inducing apoptosis or necrosis and progressing to inflammation.

Ethanol disrupts liver metabolic activity in cholemic mice

The ethanol exposure impacts various hepatic metabolic processes beyond lipids, including the modulation of several amino acids,[32] proteins,[33] carbohydrates,[34] and bile acid.[35] To comprehensively understand the consequence of alcohol consumption under conditions of elevated serum TBA, we investigated the alterations in hydrophilic compounds within liver tissues using ^{1}H NMR and hepatic bile acid via LC-MS. Our analysis revealed significant changes in the levels of hepatic metabolites linked to alcoholic steatotic liver disease. Notably, the level of adenosine monophosphate (AMP) was specifically decreased in the hTBA+Alc group compared to other groups (Figure 7A). Moreover, we observed significantly decreased glucose levels in the hTBA+Alc group compared to other groups (Figure 7B). Glutamate, a metabolite involved in the production of free ammonia (a hepatotoxic molecule), showed a marked elevation in the hTBA+Alc group (Figure 7C). Furthermore, hypoxanthine, a purine derivative that consumes NAD^+,[36] was notably higher in the hTBA+Alc group (Figure 7D). Hepatic 3-hydroxybutyrate levels were also increased in the hTBA+Alc group (Figure 7E). Remarkably, mannose levels were significantly decreased by ethanol feeding in both the nTBA and hTBA groups (Figure 7F). Hydrophilic compounds in the female mice cohort followed a similar pattern, indicating identical metabolic activity changes. These changes included decreased glucose and mannose levels (Figures 8B and F) and increased levels of glutamate and hypoxanthine (Figures 8C and 8D). The female hTBA+Alc group showed a decreasing trend in hepatic AMP and an increasing trend in 3-hydroxybutyrate levels (Figures 8A and 8E). However, these differences did not reach statistical significance compared to their respective controls. Interestingly, the levels of hepatic bile acids, including primary and secondary bile acids, were comparable among all groups in male mice (Figure S6), suggesting that the observed elevation in liver dysfunction markers in the hTBA group was not primarily driven by differences in hepatic bile acid concentrations.

DISCUSSION

Chronic and binge drinking are prevalent patterns of alcohol abuse, characterized by excessive alcohol consumption that can lead to a cascade of health problems, including liver dysfunction and even mortality.[37] The initial phase of liver impairment due to chronic alcohol consumption manifests as steatotic liver, progressing through inflammation, apoptosis, fibrosis, and finally culminating in the advanced stage of cirrhosis. Cholemia is a condition characterized by elevated serum TBAs observed in humans, including patients with AALD.[38] Although various physiological and pathological conditions like cholestasis of pregnancy and acute hepatitis can raise serum bile acid levels, the extent to which this elevation contributes to liver dysfunction during ethanol consumption remains largely unknown. Present study demonstrated that pre-existing cholemia predisposes mice to ethanol-induced liver dysfunction. Notably, the chronic ethanol intervention regime used in the current study specifically triggered hepatic dysfunction in mice with high serum TBA, highlighting that substantially elevated serum TBA accelerates the development of AALD. Existing literature suggests sex-specific differences in the consequences of alcoholic liver injury.[21,22,39] Hence, we extended our inquiry to female cholemic mice and observed similar effects.

Hepatic steatosis is the first manifestation of alcoholic liver injury and is characterized by the excessive deposit of fat inside the liver cells.[40] In the liver, there are two major ways of alcohol metabolism: alcohol dehydrogenase and cytochrome P-450 2E1 (CYP2E1). Alcohol dehydrogenase (ADH) is an enzyme in hepatocyte, which converts alcohol into acetaldehyde and further metabolized to acetate by the mitochondrial enzyme acetaldehyde dehydrogenase (ALDH). The CYP2E1 pathway metabolizes only about 10% of alcohol at normal state; however, its activity increases with increased blood alcohol concentration.[33] Both of these pathways are linked to the reduction of NAD^+ to NADH, causing elevation in the NADH/NAD^+ ratio. This imbalance significantly influences the hepatic carbohydrate and lipid metabolism.[25] Specifically, this leads to inhibited gluconeogenesis, diverting acetyl-CoA away from the Krebs cycle toward ketogenesis and *de novo* lipogenesis.[41,42] Along with inhibition of mitochondrial β-oxidation, these changes contribute to hepatic steatosis.[43,44] In our study, we observed significantly elevated hepatic triglycerides, total cholesterol, and saturated fatty acids specifically in the hTBA group, consistent with the known effects of chronic alcohol consumption on the liver.[45,46] Interestingly, we also observed significant elevation of unsaturated fatty acids including

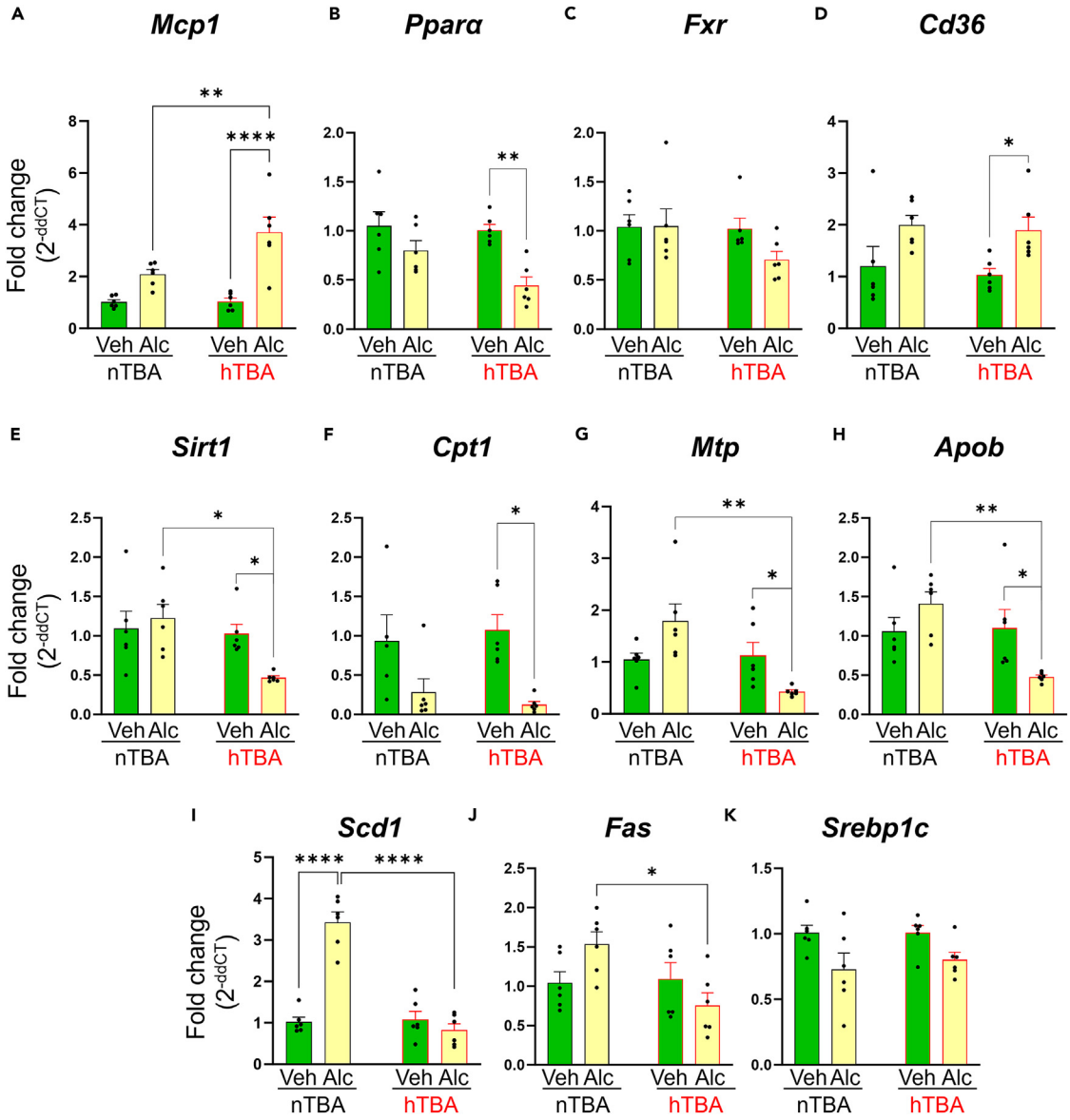

Figure 5. Ethanol consumption alters genes related to lipid metabolism in male mice with high TBA

Hepatic expressions of (A) *Mcp1*, (B) *Pparα*, (C) *Fxr*, (D) *Cd36*, (E) *Sirt1*, (F) *Cpt1*, (G) *Mtp*, (H) *Apob*, (I) *Scd1*, (J) *Fas*, and (K) *Srebp1c*. (Mcp1, monocyte chemoattractant protein-1; Pparα, peroxisome proliferator-activated receptor α; Fxr, farnesoid X receptor; Cd36, cluster of differentiation 36; Sirt1, Sirtuin 1; Cpt1, carnitine palmitoyltransferase 1; Mtp: microsomal triglyceride transfer protein; Apob: apolipoprotein B; Scd1: stearoyl-CoA desaturase 1; Fas: fatty acid synthase; Srebp1c: sterol regulatory element-binding protein 1). Data are represented as mean ± SEM (n = 5–6 mice/group, *$p < 0.05$, **$p < 0.01$, ***$p < 0.001$, ****$p < 0.0001$ by ANOVA with Tukey's post hoc test).

MUFAs and different types of PUFAs such as DHA (type of ω-3 fatty acid) and linoleic acid (type of ω-6 fatty acid), which are generally considered as healthy fats. However, the role of ω-3 fatty acids in AALD has been controversial, with reports of both protective[47–49] and exacerbating[50,51] liver dysfunction. Interestingly, total PUFA levels were not significantly different among groups in our study. Triglycerides are the predominant forms of lipids accumulated in the liver and are produced in large amounts due to the alcohol's effect on lipid metabolism. Alcohol abuse causes lipolysis in the adipose tissue by inhibiting lipogenic response of adipocytes to insulin[52] and catecholamines release,[53] which increases non-esterified fatty acids in the circulation, thereby facilitating increased hepatic fatty acid uptake via fatty acid transporters. In our study, we observed increased expression of fatty acid scavenger receptor, *Cd36*, consistent with its known role in alcohol-induced steatotic liver disease.[54]

Most significant effect of alcohol that initiates hepatic steatosis is through inhibition of mitochondrial β-oxidation process.[55,56] Various factors such as increase in NADH/NAD^+ ratio[43] and inhibition of carnitine palmitoyltransferase 1 (CPT1) activity, an enzyme crucial for

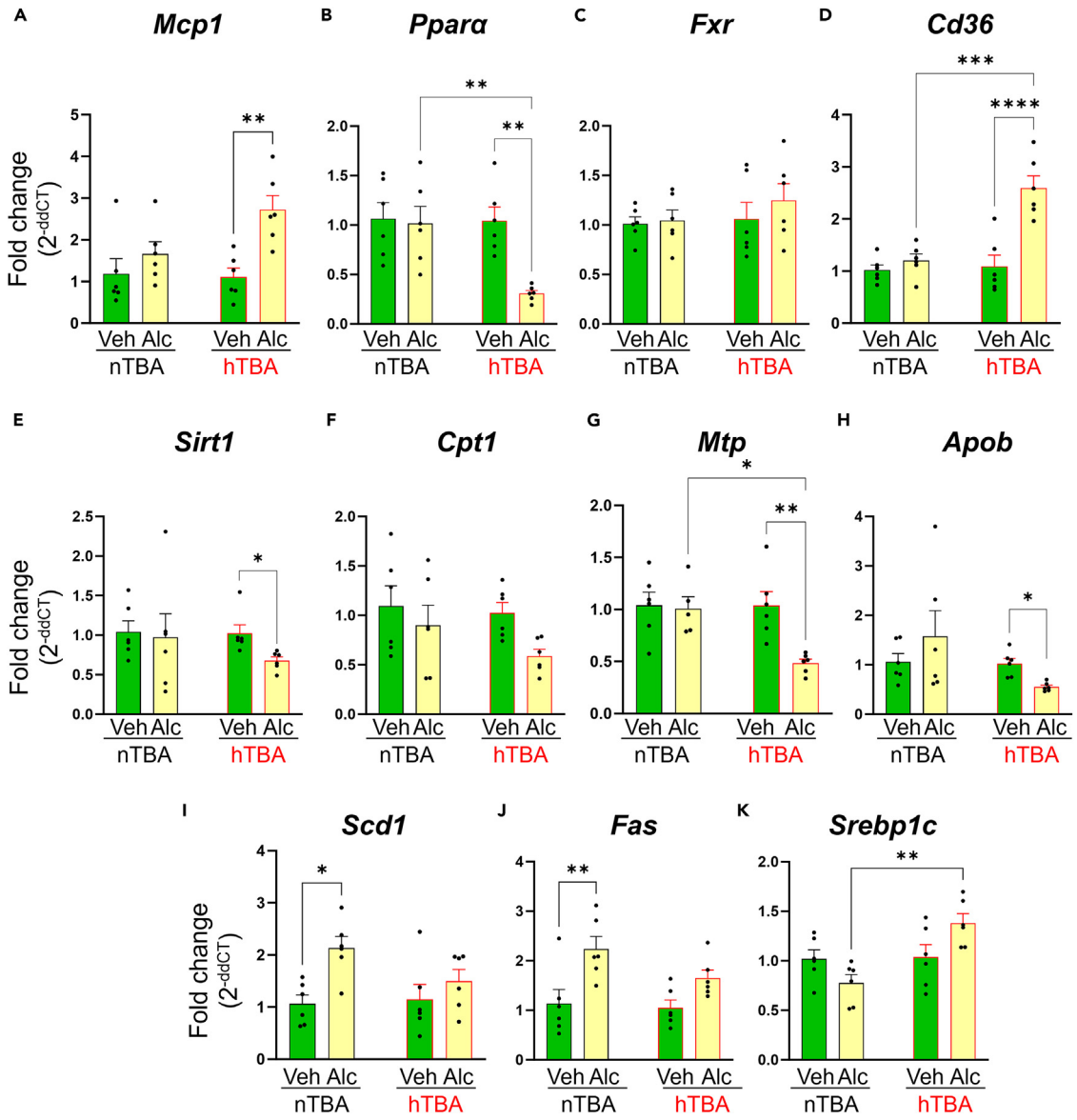

Figure 6. Ethanol consumption modifies lipid-metabolism-related genes in female mice with cholemia

Hepatic expressions of (A) *Mcp1*, (B) *Pparα*, (C) *Fxr*, (D) *Cd36*, (E) *Sirt1*, (F) *Cpt1*, (G) *Mtp*, (H) *Apob*, (I) *Scd1*, (J) *Fas*, and (K) *Srebp1c*. (Mcp1: monocyte chemoattractant protein-1; Pparα: peroxisome proliferator-activated receptor α; Fxr: farnesoid X receptor; Cd36: cluster of differentiation 36; Sirt1: Sirtuin 1; Cpt1: carnitine palmitoyltransferase 1; Mtp: microsomal triglyceride transfer protein; Apob: apolipoprotein B; Scd1: stearoyl-CoA desaturase 1; Fas: fatty acid synthase; Srebp1c: sterol regulatory element-binding protein 1). Data are represented as mean ± SEM (n = 5–6 mice/group, *p < 0.05, **p < 0.01, ***p < 0.001, ****p < 0.0001 by ANOVA with Tukey's post hoc test).

mitochondrial β-oxidation via reduced AMP-activated protein kinase (AMPK) activity,[57] inhibit the β-oxidation process. Peroxisome-proliferator-activated receptor alpha (Pparα) is a nuclear receptor that functions as a transcriptional regulator of many genes involved in mitochondrial β-oxidation, and alcohol suppresses the Pparα signaling by decreasing Pparα binding activity, thereby decreasing AMPK activity.[57] In hepatic lipid metabolism, the interdependent regulation of AMPK and Sirtuin 1 (Sirt1), a recognizer of NAD^+, is well established where Sirt1 expression stimulates the activity of AMPK and AMPK increases the NAD^+ levels, which subsequently activates Sirt1.[58] Chronic alcohol consumption is shown to impair the Sirt1-AMPK axis and mitochondrial β-oxidation process. In our study, mice with cholemia exposed to ethanol showed decreased hepatic mRNA transcripts of *Sirt1*, *Cpt1*, and *Pparα*, suggesting that compromised Sirt1 signaling and diminished β-oxidation activity may have mediated ethanol-induced hepatic steatosis in both male and female mice.

Chronic alcohol abuse has been shown to heighten the activities of enzymes associated with *de novo* lipogenesis, including stearoyl-CoA desaturase 1 (*Scd1*) and fatty acid synthase (*Fas*) mediated by the increased expression of transcription factor

Table 1. Primer sequences

Target genes	Forward (5′—3′)	Reverse (5′—3′)	Reference
36B4	*GAAAGAAGCCGAGGACCAC*	*TCTGTCACCGCCTTACCAAT*	Singh et al.[74]
Mcp1	*ATCCCAATGAGTAGGCTGGAGAGC*	*CAGAAGTGCTTGAGGTGGTTGTG*	Singh et al.[73]
Pparα	*TCACAAGTGCCTGTCTGTCG*	*CAGGTAGGCTTCGTGGATTC*	Battiprolu et al.[75]
Fxr	*GAAAGAGTGGTATCTCTGATGAG*	*ACCGCCTCTCTGTCCTTGATG*	Liu et al.[76]
Cd36	*GGAACTGTGGGCTCATTGC*	*CATGAGAATGCCTCCAAACAC*	Zhou et al.[54]
Sirt1	*ATCGGCTACCGAGACAAC*	*GTCACTAGAGCTGGCGTGT*	Cai et al.[31]
Cpt1	*TTGCACGAGGGAAAAATAAGC*	*CCCTGCATGCGGTGGAAAAGGC*	Kim et al.[77]
Mtp	*GAGCGGTCTGGATTTACAACG*	*GTAGGTAGTGACAGATGTGGCTTTTG*	Kim et al.[77]
Apob	*TCACCCCCGGGATCAAG*	*TCCAAGGACACAGAGGGCTTT*	Kim et al.[77]
Scd1	*CCGGAGACCCTTAGATCGA*	*TAGCCTGTAAAAGATTTCTGCAAACC*	Singh et al.[78]
Srebp1c	*GGTTTTGAACGACATCGAAGA*	*CGGGAAGTCACTGTCTTGGT*	Goand et al.[79]
Fas	*CGGAAACTTCAGGAAATGTCC*	*TCAGAGACGTGTCACTCCTGG*	Goand et al.[79]

Srebp1c.[59,60] In agreement, nTBA+Alc group displayed increased expression of *Scd1* (in both male and female groups) and *Fas* (female only) (Figures 5 and 6). Surprisingly, hTBA+ Alc group displayed reduced *Scd1* and *Fas* expression, specifically in male mice cohort (Figure 5), despite increased hepatic lipid accumulation. However, we observed a decrease in hepatic expression of the lipid transport genes microsomal triglyceride transfer protein (*Mtp*) and apolipoprotein-B (*Apob*), both known to be regulated by *Pparα*.[61,62] Consistent with this observation, we also found reduced hepatic expression of *Pparα*. *Mcp1*, a pro-inflammatory chemokine that has been reported to inhibit the *Pparα* activity,[27,63] was found elevated in ethanol-fed cholemic groups. Moreover, studies have reported a link between *Mcp1* and disrupted hepatic lipid regulation.[29,30] Altogether, increased accumulation of hepatic lipid in response to ethanol exposure in hTBA mice partly attributed to heightened fatty acid uptake, suppressed mitochondrial β-oxidation, and impeded export of hepatic lipids. The elevated *Mcp1* expression also suggests hepatic inflammation. However, we did not observe any notable differences in hepatic levels of TNF-α and IL-1β. Notably, the hepatic level of lipocalin 2 (Lcn2), an acute-phase protein, was significantly increased in the ethanol-fed high-TBA group. This observation aligns with a previous study demonstrating the detrimental role of Lcn2 in AALD.[31]

Rodent models of alcohol-induced liver disease reveal sex-specific differences in disease susceptibility, with female mice being more prone to developing AALD.[21] However, we did not observe a significant difference between male and female mice with elevated bile acids (high TBA) in their susceptibility to AALD. This suggests that the primary mechanisms driving liver injury in these mice, such as impaired fatty acid β-oxidation and very low-density lipoprotein (VLDL) excretion, may have masked potential sex differences in response to alcohol. Dysregulation of bile acids itself could also contribute to making both sexes susceptible to AALD.

An elevated NADH/NAD^+ ratio not only impacts lipid metabolism but also impedes carbohydrate metabolism by inhibiting gluconeogenesis through the reduction of pyruvate's steady-state concentration.[64] Consequently, acetyl-CoA is diverted toward ketogenesis and lipogenesis, bypassing entry into the Krebs cycle. The quantification of hydrophilic compounds in the liver revealed a notable decrease in glucose levels, suggesting compromised gluconeogenesis in the ethanol-fed high TBA group compared to the other three groups. This decrease in hepatic glucose could be due to increase in the NADH to NAD+ ratio, which leads to a reduction in hepatic gluconeogenesis through a decrease in pyruvate, which lowers pyruvate carboxylase activity.[64] However, this possibility requires further investigation in our future studies. Consistent with previous research,[36,65,66] we observed a significant increase in glutamate, hypoxanthine, and 3-hydroxybutyrate, a major ketone body in the liver, in the hTBA+ Alc group. Furthermore, hepatic AMP and mannose levels were significantly reduced, particularly in ethanol-fed mice with elevated serum TBA. AMP is a crucial regulator of AMPK activity,[67] whereas mannose prevents ethanol-mediated suppression of hepatic β-oxidation.[68] Collectively, these observations suggest that ethanol-induced metabolic shifts might have contributed to alcoholic steatotic liver development in mice with cholemia.

Altogether, our study demonstrates that elevated systemic bile acid increases susceptibility to alcohol-induced liver dysfunction by impairing hepatic β-oxidation and lipid transport and by shifting liver metabolism toward steatosis. This finding highlights the importance of proactive serum bile acid testing for identifying individuals at risk for early hepatic dysfunction upon alcohol consumption.

Limitations of the study

The gut microbiome is increasingly recognized as a critical modulator of liver function by exerting profound influence on bile acid metabolism. This study did not elucidate the contributory role of the gut microbiota, particularly in the context of pre-existing cholemia, in increasing susceptibility to AALD. Our future research will delve deeper into the complex interplay between the gut microbiome, ethanol exposure, and bile acid metabolism in the development of AALD in mice with elevated bile acid levels. Moreover, although we identified that ethanol feeding elevated hepatic steatosis by impairing hepatic β-oxidation and lipid transport, the underlying mechanisms primarily deduced from alterations in hepatic mRNA transcript levels. These mechanistic pathways require further confirmation through protein expression and enzymatic

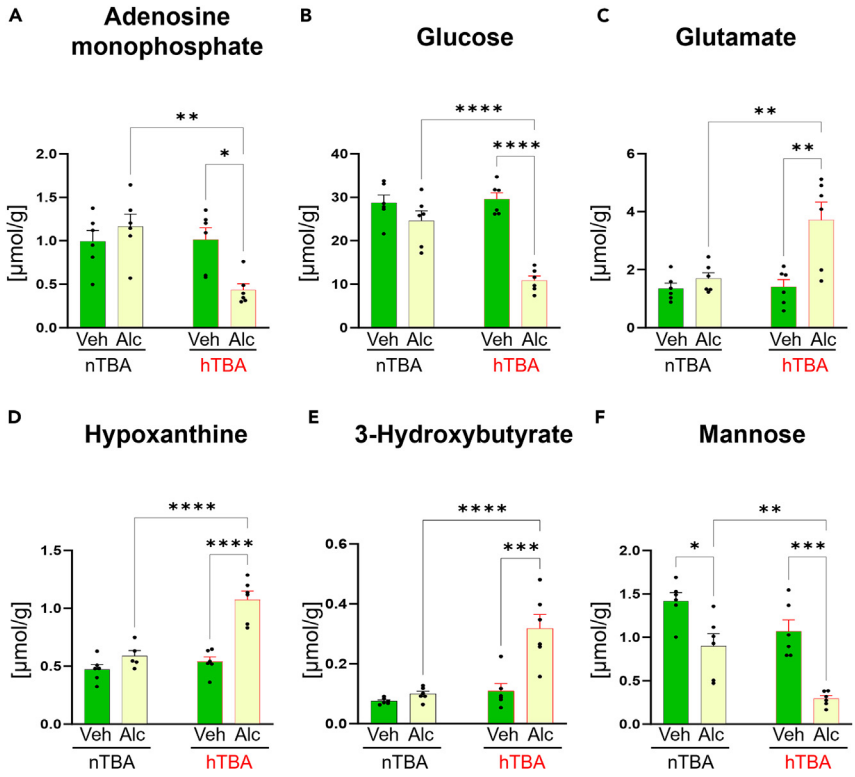

Figure 7. Ethanol consumption disrupts hepatic metabolic activity in male mice

Hepatic levels of (A) adenosine monophosphate, (B) glucose, (C) glutamate, (D) hypoxanthine, (E) 3-hydroxybutyrate, and (F) mannose. Data are represented as mean ± SEM (n = 6 mice/group, *p < 0.05, **p < 0.01, ***p < 0.001, ****p < 0.0001 by ANOVA with Tukey's post hoc test).

activity assays. Studies have shown that the selection of euthanasia techniques in rodents can affect metabolic factors, leading to elevated serum triglyceride levels, glycogen breakdown, and glucose utilization.[69,70] This can potentially overestimate serum and liver parameters, posing a limitation in our study. However, since all experimental groups were euthanized using CO_2, the influence of the euthanasia method would likely be consistent across all groups, mitigating its effect on comparisons between the groups.

RESOURCE AVAILABILITY

Lead contact

Further information and requests for resources and reagents should be directed to and will be fulfilled by the lead contact, Vishal Singh (vxs28@psu.edu).

Materials availability

This study did not generate new unique reagents.

Data and code availability

- **Data:** all data reported in this paper will be made available by the lead contact upon request.
- **Code:** this study did not use code for data analysis.
- **Additional Information:** any additional information needed for data presented in this paper is available from the lead contact upon request.

ACKNOWLEDGMENTS

D.P. was supported by the NIH training grant T32DK120509.

AUTHOR CONTRIBUTIONS

D.P. and V.S. conceived and designed the study. L.V.N., Jr. and U.K.G. helped with biochemical and histochemical assays. D.P., S.T., and A.M.K. III. conducted animal experiments and contributed to sample collection and data acquisition. F.H., Y.T., and A.D.P. contributed to ^{1}H NMR-based hepatic metabolite and bile acid analysis. A.D.P. assisted with metabolite data interpretation and manuscript writing. D.P. and V.S. analyzed and interpreted the data and wrote the manuscript.

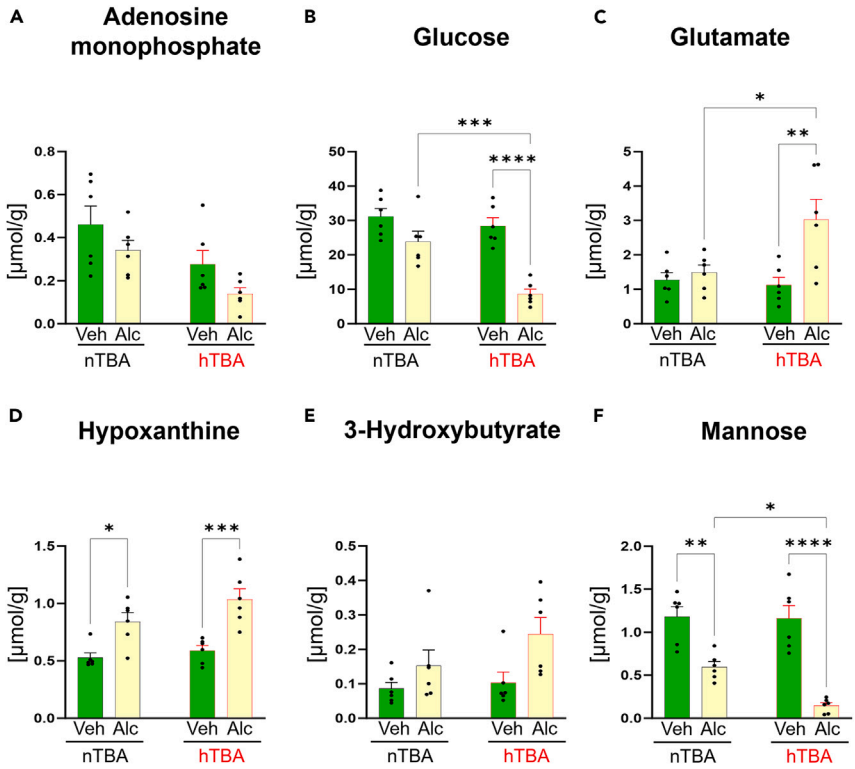

Figure 8. Ethanol consumption interferes with liver metabolic function in female mice with elevated TBA

Hepatic levels of (A) adenosine monophosphate, (B) glucose, (C) glutamate, (D) hypoxanthine, (E) 3-hydroxybutyrate, and (F) mannose. Data are represented as mean ± SEM (n = 6 mice/group, *p < 0.05, **p < 0.01, ***p < 0.001, ****p < 0.0001 by ANOVA with Tukey's post hoc test).

DECLARATION OF INTERESTS

The authors declare that they have no competing interests.

STAR★METHODS

Detailed methods are provided in the online version of this paper and include the following:

- KEY RESOURCES TABLE
- EXPERIMENTAL MODEL AND STUDY PARTICIPANT DETAILS
  - Mice and diets
- METHOD DETAILS
  - Serum total bile acid (TBA) analysis
  - Chronic binge ethanol feeding
  - National institute on alcohol abuse and alcoholism (NIAAA) model of ethanol administration
  - Mouse euthanasia and sample collection
  - Serum biochemical analysis
  - Enzyme linked immunosorbent assay (ELISA)
  - RNA isolation, cDNA preparation and quantitative reverse transcription polymerase chain reaction
  - Histochemical and terminal deoxynucleotidyl transferase dUTP nick end labeling (TUNEL) staining
  - Quantitative assessment of hepatic lipids and hydrophilic compounds by ^{1}H NMR
  - Liver bile acid analysis
- QUANTIFICATION AND STATISTICAL ANALYSIS

SUPPLEMENTAL INFORMATION

Supplemental information can be found online at https://doi.org/10.1016/j.isci.2024.110940.

Received: January 29, 2024
Revised: June 21, 2024
Accepted: September 10, 2024
Published: September 13, 2024

REFERENCES

1. GBD 2016 Alcohol Collaborators (2018). Alcohol use and burden for 195 countries and territories, 1990-2016: a systematic analysis for the Global Burden of Disease Study 2016. Lancet *392*, 1015–1035. https://doi.org/10.1016/S0140-6736(18)31310-2.
2. Drinking Levels, Patterns Defined (2024). National Institute on Alcohol Abuse and Alcoholism. https://www.niaaa.nih.gov/alcohol-health/overview-alcohol-consumption/moderate-binge-drinking.
3. Bohm, M.K., Liu, Y., Esser, M.B., Mesnick, J.B., Lu, H., Pan, Y., and Greenlund, K.J. (2021). Binge Drinking Among Adults, by Select Characteristics and State - United States, 2018. MMWR Morb. Mortal. Wkly. Rep. *70*, 1441–1446. https://doi.org/10.15585/mmwr.mm7041a2.
4. Understanding Binge Drinking (2021). National Institute on Alcohol Abuse and Alcholism (NIAAA), p. 1. https://www.niaaa.nih.gov/publications/brochures-and-fact-sheets/binge-drinking.
5. Majsterek, M., Wierzchowska-Opoka, M., Makosz, I., Kreczyńska, L., Kimber-Trojnar, Ż., and Leszczyńska-Gorzelak, B. (2022). Bile Acids in Intrahepatic Cholestasis of Pregnancy. Diagnostics *12*, 2746. https://doi.org/10.3390/diagnostics12112746.
6. Li, Y., Deng, X., Zhou, H., Zheng, X., Zhang, G., and Xiong, Q. (2023). Bile acid predicts congenital portosystemic venous shunt in patients with pulmonary arterial hypertension. Eur. J. Med. Res. *28*, 74. https://doi.org/10.1186/s40001-023-01039-0.
7. Xu, S., Zhang, P., Hu, L., Zhou, W., and Cheng, G. (2021). Case Report: Clinical Features of Congenital Portosystemic Shunts in the Neonatal Period. Front. Pediatr. *9*, 778791. https://doi.org/10.3389/fped.2021.778791.
8. Kim, M.J., and Suh, D.J. (1986). Profiles of serum bile acids in liver diseases. Korean J. Intern. Med. *1*, 37–42. https://doi.org/10.3904/kjim.1986.1.1.37.
9. Geenes, V., and Williamson, C. (2009). Intrahepatic cholestasis of pregnancy. World J. Gastroenterol. *15*, 2049–2066. https://doi.org/10.3748/wjg.15.2049.
10. Sahni, A., and Jogdand, S.D. (2022). Effects of Intrahepatic Cholestasis on the Foetus During Pregnancy. Cureus *14*, e30657. https://doi.org/10.7759/cureus.30657.
11. Robinson, E.B., Jordan, G., Katz, D., Sundaram, S.S., Boster, J., Brigham, D., Ladd, P., Chan, C.M., Shay, R.L., Ochmanek, E., and Annam, A. (2023). Congenital Portosystemic Shunts: Variable Clinical Presentations Requiring a Tailored Endovascular or Surgical Approach. JPGN Rep. *4*, e279. https://doi.org/10.1097/PG9.0000000000000279.
12. de Martinis, L., Groppelli, G., Corti, R., Moramarco, L.P., Quaretti, P., De Cata, P., Rotondi, M., and Chiovato, L. (2017). Disabling portosystemic encephalopathy in a non-cirrhotic patient: Successful endovascular treatment of a giant inferior mesenteric-caval shunt. World J. Gastroenterol. *23*, 8426–8431. https://doi.org/10.3748/wjg.v23.i47.8426.
13. Nardelli, S., Riggio, O., Turco, L., Gioia, S., Puzzono, M., Bianchini, M., Ridola, L., Aprile, F., Gitto, S., Pelle, G., et al. (2021). Relevance of Spontaneous Portosystemic Shunts Detected with CT in Patients with Cirrhosis. Radiology *299*, 133–140. https://doi.org/10.1148/radiol.2021203051.
14. Lin, Z.Y., Chen, S.C., Hsieh, M.Y., Wang, C.W., Chuang, W.L., and Wang, L.Y. (2006). Incidence and clinical significance of spontaneous intrahepatic portosystemic venous shunts detected by sonography in adults without potential cause. J. Clin. Ultrasound *34*, 22–26. https://doi.org/10.1002/jcu.20176.
15. Bernard, O., Franchi-Abella, S., Branchereau, S., Pariente, D., Gauthier, F., and Jacquemin, E. (2012). Congenital portosystemic shunts in children: recognition, evaluation, and management. Semin. Liver Dis. *32*, 273–287. https://doi.org/10.1055/s-0032-1329896.
16. Papamichail, M., Pizanias, M., and Heaton, N. (2018). Congenital portosystemic venous shunt. Eur. J. Pediatr. *177*, 285–294. https://doi.org/10.1007/s00431-017-3058-x.
17. Farooqui, N., and Elhence, A.; Shalimar (2022). A Current Understanding of Bile Acids in Chronic Liver Disease. J. Clin. Exp. Hepatol. *12*, 155–173. https://doi.org/10.1016/j.jceh.2021.08.017.
18. Chiang, J.Y.L., and Ferrell, J.M. (2018). Bile Acid Metabolism in Liver Pathobiology. Gene Expr. *18*, 71–87. https://doi.org/10.3727/105221618X15156018385515.
19. Javitt, N.B. (2020). Hepatic bile formation: bile acid transport and water flow into the canalicular conduit. Am. J. Physiol. Gastrointest. Liver Physiol. *319*, G609–G618. https://doi.org/10.1152/ajpgi.00078.2020.
20. Yeoh, B.S., Golonka, R.M., Saha, P., Kandalgaonkar, M.R., Tian, Y., Osman, I., Patterson, A.D., Gewirtz, A.T., Joe, B., and Vijay-Kumar, M. (2023). Urine-based Detection of Congenital Portosystemic Shunt in C57BL/6 Mice. Function (Oxf) *4*, zqad040. https://doi.org/10.1093/function/zqad040.
21. Wagnerberger, S., Fiederlein, L., Kanuri, G., Stahl, C., Millonig, G., Mueller, S., Bischoff, S.C., and Bergheim, I. (2013). Sex-specific differences in the development of acute alcohol-induced liver steatosis in mice. Alcohol Alcohol *48*, 648–656. https://doi.org/10.1093/alcalc/agt138.
22. Li, S.Q., Wang, P., Wang, D.M., Lu, H.J., Li, R.F., Duan, L.X., Zhu, S., Wang, S.L., Zhang, Y.Y., and Wang, Y.L. (2019). Molecular mechanism for the influence of gender dimorphism on alcoholic liver injury in mice. Hum. Exp. Toxicol. *38*, 65–81. https://doi.org/10.1177/0960327118777869.
23. Brandl, K., Hartmann, P., Jih, L.J., Pizzo, D.P., Argemi, J., Ventura-Cots, M., Coulter, S., Liddle, C., Ling, L., Rossi, S.J., et al. (2018). Dysregulation of serum bile acids and FGF19 in alcoholic hepatitis. J. Hepatol. *69*, 396–405. https://doi.org/10.1016/j.jhep.2018.03.031.
24. Bertola, A., Mathews, S., Ki, S.H., Wang, H., and Gao, B. (2013). Mouse model of chronic and binge ethanol feeding (the NIAAA model). Nat. Protoc. *8*, 627–637. https://doi.org/10.1038/nprot.2013.032.
25. You, M., and Arteel, G.E. (2019). Effect of ethanol on lipid metabolism. J. Hepatol. *70*, 237–248. https://doi.org/10.1016/j.jhep.2018.10.037.
26. Osipova, D., Kokoreva, K., Lazebnik, L., Golovanova, E., Pavlov, C., Dukhanin, A., Orlova, S., and Starostin, K. (2022). Regression of Liver Steatosis Following Phosphatidylcholine Administration: A Review of Molecular and Metabolic Pathways Involved. Front. Pharmacol. *13*, 797923. https://doi.org/10.3389/fphar.2022.797923.
27. Mandrekar, P., Ambade, A., Lim, A., Szabo, G., and Catalano, D. (2011). An essential role for monocyte chemoattractant protein-1 in alcoholic liver injury: regulation of proinflammatory cytokines and hepatic steatosis in mice. Hepatology *54*, 2185–2197. https://doi.org/10.1002/hep.24599.
28. Czaja, M.J., Geerts, A., Xu, J., Schmiedeberg, P., and Ju, Y. (1994). Monocyte chemoattractant protein 1 (MCP-1) expression occurs in toxic rat liver injury and human liver disease. J. Leukoc. Biol. *55*, 120–126. https://doi.org/10.1002/jlb.55.1.120.
29. Clément, S., Juge-Aubry, C., Sgroi, A., Conzelmann, S., Pazienza, V., Pittet-Cuenod, B., Meier, C.A., and Negro, F. (2008). Monocyte chemoattractant protein-1 secreted by adipose tissue induces direct lipid accumulation in hepatocytes. Hepatology *48*, 799–807. https://doi.org/10.1002/hep.22404.
30. Kanda, H., Tateya, S., Tamori, Y., Kotani, K., Hiasa, K.i., Kitazawa, R., Kitazawa, S., Miyachi, H., Maeda, S., Egashira, K., and Kasuga, M. (2006). MCP-1 contributes to macrophage infiltration into adipose tissue, insulin resistance, and hepatic steatosis in obesity. J. Clin. Invest. *116*, 1494–1505. https://doi.org/10.1172/JCI26498.
31. Cai, Y., Jogasuria, A., Yin, H., Xu, M.J., Hu, X., Wang, J., Kim, C., Wu, J., Lee, K., Gao, B., and You, M. (2016). The Detrimental Role Played by Lipocalin-2 in Alcoholic Fatty Liver in Mice. Am. J. Pathol. *186*, 2417–2428. https://doi.org/10.1016/j.ajpath.2016.05.006.
32. Mrdjen, M., Huang, E., Pathak, V., Bellar, A., Welch, N., Dasarathy, J., Streem, D., McClain, C.J., Mitchell, M., Radaeva, S., et al. (2023). Dysregulated meta-organismal metabolism of aromatic amino acids in alcohol-associated liver disease. Hepatol. Commun. *7*, e0284. https://doi.org/10.1097/HC9.0000000000000284.
33. Zakhari, S. (2006). Overview: how is alcohol metabolized by the body? Alcohol Res. Health *29*, 245–254.
34. Rehfeld, J.F., Juhl, E., and Hilden, M. (1973). Carbohydrate metabolism in alcohol-induced fatty liver. Evidence for an abnormal insulin response to glucagon in alcoholic liver disease. Gastroenterology *64*, 445–451.
35. Nilsson, L.M., Sjövall, J., Strom, S., Bodin, K., Nowak, G., Einarsson, C., and Ellis, E. (2007). Ethanol stimulates bile acid formation in primary human hepatocytes. Biochem. Biophys. Res. Commun. *364*, 743–747. https://doi.org/10.1016/j.bbrc.2007.10.039.
36. Toledo-Ibelles, P., Gutiérrez-Vidal, R., Calixto-Tlacomulco, S., Delgado-Coello, B., and Mas-Oliva, J. (2021). Hepatic Accumulation of Hypoxanthine: A Link Between Hyperuricemia and Nonalcoholic Fatty Liver Disease. Arch. Med. Res. *52*, 692–702. https://doi.org/10.1016/j.arcmed.2021.04.005.
37. Esser, M.B., Sherk, A., Liu, Y., Naimi, T.S., Stockwell, T., Stahre, M., Kanny, D., Landen, M., Saitz, R., and Brewer, R.D. (2020). Deaths and Years of Potential Life Lost From Excessive Alcohol Use - United States, 2011-2015. MMWR Morb. Mortal. Wkly. Rep. *69*,

1428–1433. https://doi.org/10.15585/mmwr.mm6939a6.
38. Tung, B.Y., and Carithers, R.L. (1999). Cholestasis and alcoholic liver disease. Clin. Liver Dis. *3*, 585–601. https://doi.org/10.1016/s1089-3261(05)70086-6.
39. Wilkin, R.J.W., Lalor, P.F., Parker, R., and Newsome, P.N. (2016). Murine Models of Acute Alcoholic Hepatitis and Their Relevance to Human Disease. Am. J. Pathol. *186*, 748–760. https://doi.org/10.1016/j.ajpath.2015.12.003.
40. French, S.W. (1996). Ethanol and hepatocellular injury. Clin. Lab. Med. *16*, 289–306.
41. Siler, S.Q., Neese, R.A., Christiansen, M.P., and Hellerstein, M.K. (1998). The inhibition of gluconeogenesis following alcohol in humans. Am. J. Physiol. *275*, E897–E907. https://doi.org/10.1152/ajpendo.1998.275.5.E897.
42. Cederbaum, A.I. (2012). Alcohol metabolism. Clin. Liver Dis. *16*, 667–685. https://doi.org/10.1016/j.cld.2012.08.002.
43. Grunnet, N., and Kondrup, J. (1986). The effect of ethanol on the beta-oxidation of fatty acids. Alcohol Clin. Exp. Res. *10*, 64S–68S. https://doi.org/10.1111/j.1530-0277.1986.tb05182.x.
44. Lieber, C.S. (1991). Hepatic, metabolic and toxic effects of ethanol: 1991 update. Alcohol Clin. Exp. Res. *15*, 573–592. https://doi.org/10.1111/j.1530-0277.1991.tb00563.x.
45. Sozio, M., and Crabb, D.W. (2008). Alcohol and lipid metabolism. Am. J. Physiol. Endocrinol. Metab. *295*, E10–E16. https://doi.org/10.1152/ajpendo.00011.2008.
46. Sabesin, S.M. (1981). Lipid and lipoprotein abnormalities in alcoholic liver disease. Circulation *64*, 72–84.
47. Wang, M., Zhang, X., Ma, L.J., Feng, R.B., Yan, C., Su, H., He, C., Kang, J.X., Liu, B., and Wan, J.B. (2017). Omega-3 polyunsaturated fatty acids ameliorate ethanol-induced adipose hyperlipolysis: A mechanism for hepatoprotective effect against alcoholic liver disease. Biochim. Biophys. Acta, Mol. Basis Dis. *1863*, 3190–3201. https://doi.org/10.1016/j.bbadis.2017.08.026.
48. Wada, S., Yamazaki, T., Kawano, Y., Miura, S., and Ezaki, O. (2008). Fish oil fed prior to ethanol administration prevents acute ethanol-induced fatty liver in mice. J. Hepatol. *49*, 441–450. https://doi.org/10.1016/j.jhep.2008.04.026.
49. Wang, M., Zhang, X.J., Feng, K., He, C., Li, P., Hu, Y.J., Su, H., and Wan, J.B. (2016). Dietary α-linolenic acid-rich flaxseed oil prevents against alcoholic hepatic steatosis via ameliorating lipid homeostasis at adipose tissue-liver axis in mice. Sci. Rep. *6*, 26826. https://doi.org/10.1038/srep26826.
50. Nanji, A.A., Zhao, S., Sadrzadeh, S.M., Dannenberg, A.J., Tahan, S.R., and Waxman, D.J. (1994). Markedly enhanced cytochrome P450 2E1 induction and lipid peroxidation is associated with severe liver injury in fish oil-ethanol-fed rats. Alcohol Clin. Exp. Res. *18*, 1280–1285. https://doi.org/10.1111/j.1530-0277.1994.tb00119.x.
51. Feng, R., Ma, L.J., Wang, M., Liu, C., Yang, R., Su, H., Yang, Y., and Wan, J.B. (2020). Oxidation of fish oil exacerbates alcoholic liver disease by enhancing intestinal dysbiosis in mice. Commun. Biol. *3*, 481. https://doi.org/10.1038/s42003-020-01213-8.
52. Carr, R.M., and Correnti, J. (2015). Insulin resistance in clinical and experimental alcoholic liver disease. Ann. N. Y. Acad. Sci. *1353*, 1–20. https://doi.org/10.1111/nyas.12787.
53. Zhao, C., Liu, Y., Xiao, J., Liu, L., Chen, S., Mohammadi, M., McClain, C.J., Li, X., and Feng, W. (2015). FGF21 mediates alcohol-induced adipose tissue lipolysis by activation of systemic release of catecholamine in mice. J. Lipid Res. *56*, 1481–1491. https://doi.org/10.1194/jlr.M058610.
54. Zhou, J., Febbraio, M., Wada, T., Zhai, Y., Kuruba, R., He, J., Lee, J.H., Khadem, S., Ren, S., Li, S., et al. (2008). Hepatic fatty acid transporter Cd36 is a common target of LXR, PXR, and PPARgamma in promoting steatosis. Gastroenterology *134*, 556–567. https://doi.org/10.1053/j.gastro.2007.11.037.
55. Blomstrand, R., Kager, L., and Lantto, O. (1973). Studies on the ethanol-induced decrease of fatty acid oxidation in rat and human liver slices. Life Sci. *13*, 1131–1141. https://doi.org/10.1016/0024-3205(73)90380-9.
56. Cederbaum, A.I., Lieber, C.S., Beattie, D.S., and Rubin, E. (1975). Effect of chronic ethanol ingestion on fatty acid oxidation by hepatic mitochondria. J. Biol. Chem. *250*, 5122–5129.
57. You, M., Matsumoto, M., Pacold, C.M., Cho, W.K., and Crabb, D.W. (2004). The role of AMP-activated protein kinase in the action of ethanol in the liver. Gastroenterology *127*, 1798–1808. https://doi.org/10.1053/j.gastro.2004.09.049.
58. Jeon, S., and Carr, R. (2020). Alcohol effects on hepatic lipid metabolism. J. Lipid Res. *61*, 470–479. https://doi.org/10.1194/jlr.R119000547.
59. Foufelle, F., and Ferré, P. (2002). New perspectives in the regulation of hepatic glycolytic and lipogenic genes by insulin and glucose: a role for the transcription factor sterol regulatory element binding protein-1c. Biochem. J. *366*, 377–391. https://doi.org/10.1042/BJ20020430.
60. Liangpunsakul, S., Ross, R.A., and Crabb, D.W. (2013). Activation of carbohydrate response element-binding protein by ethanol. J. Investig. Med. *61*, 270–277. https://doi.org/10.2310/JIM.0b013e31827c2795.
61. Améen, C., Edvardsson, U., Ljungberg, A., Asp, L., Akerblad, P., Tuneld, A., Olofsson, S.O., Lindén, D., and Oscarsson, J. (2005). Activation of peroxisome proliferator-activated receptor alpha increases the expression and activity of microsomal triglyceride transfer protein in the liver. J. Biol. Chem. *280*, 1224–1229. https://doi.org/10.1074/jbc.M412107200.
62. Lindén, D., Alsterholm, M., Wennbo, H., and Oscarsson, J. (2001). PPARalpha deficiency increases secretion and serum levels of apolipoprotein B-containing lipoproteins. J. Lipid Res. *42*, 1831–1840.
63. Peng, Y., Li, Q., Zhang, L., Bai, M., and Zhang, Z. (2012). Peroxisome Proliferator-Activated Receptor α Plays an Important Role in the Expression of Monocyte Chemoattractant Protein-1 and Neointimal Hyperplasia after Vascular Injury. PPAR Res. *2012*, 970525. https://doi.org/10.1155/2012/970525.
64. Krebs, H.A., Freedland, R.A., Hems, R., and Stubbs, M. (1969). Inhibition of hepatic gluconeogenesis by ethanol. Biochem. J. *112*, 117–124. https://doi.org/10.1042/bj1120117.
65. Choi, W.M., Kim, H.H., Kim, M.H., Cinar, R., Yi, H.S., Eun, H.S., Kim, S.H., Choi, Y.J., Lee, Y.S., Kim, S.Y., et al. (2019). Glutamate Signaling in Hepatic Stellate Cells Drives Alcoholic Steatosis. Cell Metab. *30*, 877–889.e7. https://doi.org/10.1016/j.cmet.2019.08.001.
66. Rasineni, K., and Casey, C.A. (2012). Molecular mechanism of alcoholic fatty liver. Indian J. Pharmacol. *44*, 299–303. https://doi.org/10.4103/0253-7613.96297.
67. Hardie, D.G. (2004). The AMP-activated protein kinase pathway–new players upstream and downstream. J. Cell Sci. *117*, 5479–5487. https://doi.org/10.1242/jcs.01540.
68. Hu, M., Chen, Y., Deng, F., Chang, B., Luo, J., Dong, L., Lu, X., Zhang, Y., Chen, Z., and Zhou, J. (2022). D-Mannose Regulates Hepatocyte Lipid Metabolism. Front. Immunol. *13*, 877650. https://doi.org/10.3389/fimmu.2022.877650.
69. Pierozan, P., Jernerén, F., Ransome, Y., and Karlsson, O. (2017). The Choice of Euthanasia Method Affects Metabolic Serum Biomarkers. Basic Clin. Pharmacol. Toxicol. *121*, 113–118. https://doi.org/10.1111/bcpt.12774.
70. Brooks, S.P., Lampi, B.J., and Bihun, C.G. (1999). The Influence of Euthanasia Methods on Rat Liver Metabolism. Contemp. Top. Lab. Anim. Sci. *38*, 19–24.
71. Yeoh, B.S., Saha, P., Golonka, R.M., Zou, J., Petrick, J.L., Abokor, A.A., Xiao, X., Bovilla, V.R., Bretin, A.C.A., Rivera-Esteban, J., et al. (2022). Enterohepatic Shunt-Driven Cholemia Predisposes to Liver Cancer. Gastroenterology *163*, 1658–1671.e16. https://doi.org/10.1053/j.gastro.2022.08.033.
72. Gallage, S., Ali, A., Barragan Avila, J.E., Herebian, D., Karimi, M.M., Irvine, E.E., McHugh, D., Schneider, A.T., Vucur, M., Keitel, V., et al. (2022). Spontaneous Cholemia in C57BL/6 Mice Predisposes to Liver Cancer in NASH. Cell. Mol. Gastroenterol. Hepatol. *13*, 875–878. https://doi.org/10.1016/j.jcmgh.2021.11.012.
73. Singh, V., Yeoh, B.S., Chassaing, B., Xiao, X., Saha, P., Aguilera Olvera, R., Lapek, J.D., Jr., Zhang, L., Wang, W.B., Hao, S., et al. (2018). Dysregulated Microbial Fermentation of Soluble Fiber Induces Cholestatic Liver Cancer. Cell *175*, 679–694.e22. https://doi.org/10.1016/j.cell.2018.09.004.
74. Singh, V., Kumar, M., San Yeoh, B., Xiao, X., Saha, P., Kennett, M.J., and Vijay-Kumar, M. (2016). Inhibition of Interleukin-10 Signaling Induces Microbiota-dependent Chronic Colitis in Apolipoprotein E Deficient Mice. Inflamm. Bowel Dis. *22*, 841–852. https://doi.org/10.1097/MIB.0000000000000699.
75. Battiprolu, P.K., Hojayev, B., Jiang, N., Wang, Z.V., Luo, X., Iglewski, M., Shelton, J.M., Gerard, R.D., Rothermel, B.A., Gillette, T.G., et al. (2012). Metabolic stress-induced activation of FoxO1 triggers diabetic cardiomyopathy in mice. J. Clin. Invest. *122*, 1109–1118. https://doi.org/10.1172/JCI60329.
76. Liu, L., Zhang, L., Zhang, L., Yang, F., Zhu, X., Lu, Z., Yang, Y., Lu, H., Feng, L., Wang, Z., et al. (2017). Hepatic Tmem30a Deficiency Causes Intrahepatic Cholestasis by Impairing Expression and Localization of Bile Salt Transporters. Am. J. Pathol. *187*, 2775–2787. https://doi.org/10.1016/j.ajpath.2017.08.011.
77. Kim, H.S., Xiao, C., Wang, R.H., Lahusen, T., Xu, X., Vassilopoulos, A., Vazquez-Ortiz, G., Jeong, W.I., Park, O., Ki, S.H., et al. (2010). Hepatic-specific disruption of SIRT6 in mice results in fatty liver formation due to enhanced glycolysis and triglyceride synthesis. Cell Metab. *12*, 224–236. https://doi.org/10.1016/j.cmet.2010.06.009.

78. Singh, V., Chassaing, B., Zhang, L., San Yeoh, B., Xiao, X., Kumar, M., Baker, M.T., Cai, J., Walker, R., Borkowski, K., et al. (2015). Microbiota-Dependent Hepatic Lipogenesis Mediated by Stearoyl CoA Desaturase 1 (SCD1) Promotes Metabolic Syndrome in TLR5-Deficient Mice. Cell Metab. *22*, 983–996. https://doi.org/10.1016/j.cmet.2015.09.028.

79. Goand, U.K., Patel, I., Verma, S., Yadav, S., Maity, D., Singh, N., Vishwakarma, S., Rathaur, S., Garg, R., and Gayen, J.R. (2023). Immunometabolic impact of pancreastatin inhibitor PSTi8 in MCD induced mouse model of oxidative stress and steatohepatitis. Cytokine *171*, 156354. https://doi.org/10.1016/j.cyto.2023.156354.

80. Amiel, A., Tremblay-Franco, M., Gautier, R., Ducheix, S., Montagner, A., Polizzi, A., Debrauwer, L., Guillou, H., Bertrand-Michel, J., and Canlet, C. (2019). Proton NMR Enables the Absolute Quantification of Aqueous Metabolites and Lipid Classes in Unique Mouse Liver Samples. Metabolites *10*, 9. https://doi.org/10.3390/metabo10010009.

81. Tian, Y., Cai, J., Allman, E.L., Smith, P.B., and Patterson, A.D. (2021). Quantitative Analysis of Bile Acid with UHPLC-MS/MS. Methods Mol. Biol. *2194*, 291–300. https://doi.org/10.1007/978-1-0716-0849-4_15.

STAR★METHODS

KEY RESOURCES TABLE

REAGENT or RESOURCE	SOURCE	IDENTIFIER
Chemicals, peptides, and recombinant proteins		
RNA Later	Sigma Life Science	Cat# R0901
qScriptUltra supermix	Quanta Bio	Cat# 95217-100
PerfeCTa SYBR® Green FastMix	Quanta Bio	Cat# 95072-250
RIPA cell lysate buffer	Sigma Life Science	Cat# R0278-500ML
3-(Trimethylsilyl) propionic-2,2,3,3-d_4 acid sodium salt	Sigma Life Science	Cat# 269913-1G
Chloroform-d (contains 0.03% TMS, v/v)	Sigma Life Science	Cat# 225789-100G
Critical commercial assays		
Total bile acid assay	Diazyme Laboratories	Cat# DZ042A-K01
RNA extraction kit	Cytiva	Cat# 25050071
BCA Protein Assay kit	Thermofisher Scientific	Cat# 23225
Mouse Tumor necrosis factor alpha (TNFα)	R&D Systems	Cat# DY410
Mouse Interleukin-1 beta (IL-1β)	R&D Systems	Cat# DY401
Mouse Lipocalin-2/NGAL Duoset	R&D Systems	Cat# DY1857
One-step TUNEL *In Situ* Apoptosis Kit	Elabscience	Cat# E-CK-A324
Experimental models: Organisms/strains		
C57BL/6 WT Mice	Animal facility: The Pennsylvania State University (PSU) and The Jackson Laboratory	Strain#: 000664
Software and algorithms		
Graphpad Prism	Graphpad	Version 10.1.2
Biorender	BioRender	www.biorender.com
Chenomx software	Chenomx Inc	www.chenomx.com

EXPERIMENTAL MODEL AND STUDY PARTICIPANT DETAILS

Mice and diets

C57BL/6J background wild-type (WT) mice, both male and female were bred and maintained under specific pathogen-free conditions at The Pennsylvania State University, University Park, Pennsylvania. Mice were housed in standard cages with corncob bedding and nestlets, with 3–4 mice per cage. Throughout the study period, mice had unrestricted access to food, water and ethanol based on the group treatment. All experimental procedures were conducted in compliance with the ethical guidelines and standards approved by the Institutional Animal Care and Use Committee at The Pennsylvania State University (protocol #: PROTO202101953). The minimum required number of mice per genotype to achieve statistically significant results was 5–7 and was determined through sample size calculation, using a significance level (α) of 0.05 and a statistical power (β) of 0.80.

METHOD DETAILS

Serum total bile acid (TBA) analysis

The concentration of serum total bile acids served as an indicator for cholemia and portosystemic shunt.[20,71,72] Blood was collected from mice one-week post-weaning via submandibular bleeding into serum separator tubes. The serum was isolated after centrifugation. Subsequently, TBA level was determined in the serum samples using a TBA analysis kit (Diazyme Laboratories) according to the manufacturer's protocol.

Chronic binge ethanol feeding

For chronic binge ethanol feeding, both male and female wild-type mice (n = 5–8/group, 12 weeks old) were initially screened for serum TBA levels and categorized into two groups: normal TBA (nTBA) and high TBA (hTBA). Within each group, mice were further divided to receive either unrestricted tap water (Veh) or 20% ethanol (Alc) for 4 weeks of experimental period. After one week of habituation, all mice were

subjected to 4 weekly oral gavages with either Veh or Alc (3.2 g/kg body weight) based on their treatments. After each weekly gavage, mice were put over heating pad for 24 h to prevent hypothermia due to ethanol consumption. Continuous monitoring of the experiment's progress was maintained by recording the weekly body weights. On the day of euthanasia, each mouse in the ethanol group received a morning gavage administration of the 20% ethanol solution between 8 and 10 a.m. Subsequently, euthanasia was conducted in the evening, typically between 5 and 7 p.m., to collect pertinent tissue samples. The time interval of 8–9 h between the gavage administration and euthanasia was designed to facilitate peak liver injury, characterized by elevated levels of alanine transaminase (ALT) and aspartate transaminase (AST). To assess the impact of chronic binge drinking of alcohol on various aspects of liver injury, physiological and metabolic alterations, the expression of inflammatory cytokines, gross liver morphology, overall body weight, as well as histological staining characteristics were measured.

National institute on alcohol abuse and alcoholism (NIAAA) model of ethanol administration

Following the guideline of the National Institute on alcohol abuse and alcoholism (NIAAA) mouse model of chronic and binge ethanol feeding,[24] mice were maintained on standard chow diet until they reached 12 weeks of age. To acclimate the mice to tube feeding, they were provided with a nutritionally adequate liquid diet for 5 days. Then mice were provided with either control or 5% ethanol containing diet for a period of 11 days with *ad libitum* liquid diet feeding. The body weight was monitored daily throughout the alcohol intervention period. On the morning of the 11th day, mice in the ethanol groups were administered a single dose of ethanol [5 g/kg body weight, ~31.5% (v/v) ethanol] via oral gavage, while mice in the control groups received isocaloric dextrin maltose. After the gavage procedure, mice were placed on water heating pads to prevent hypothermia and were monitored for a minimum of 3 h to ensure proper administration, as indicated by resumption of normal behavior and movement. Approximately 9 h post-gavage, mice were euthanized when they reached peak levels of serum alanine aminotransferase (ALT) and aspartate transaminase (AST) indicating maximum levels of liver injury.

Mouse euthanasia and sample collection

Euthanasia of experimental mice was conducted using a humane method, involving exposure to carbon dioxide (CO_2). Following the euthanasia procedure, blood specimens were collected from the inferior vena cava, deposited into specialized serum separator tubes (Becton Dickinson) and centrifuged to obtain hemolysis-free serum. Liver tissue was systematically perfused with ice-cold phosphate buffered saline (PBS) and promptly transferred to a container pre-chilled with liquid nitrogen or dry ice for protein extraction. Liver tissues for RNA analysis were stored at −20°C in RNA later solution (Sigma Aldrich). For histology, liver tissue was carefully excised and subsequently immersed in neutral buffered formalin (NBF) for a 24-h fixation period. After this fixation, it was transferred to 70% ethanol and submitted to Penn State University animal diagnostic laboratory facility for embedding in paraffin blocks, generating 5μm cross-sections and for hematoxylin and eosin (H&E) staining.

Serum biochemical analysis

About 120 μL of serum aliquots were submitted to Animal Resources Program at Penn State University. Serum levels of aspartate aminotransferase (AST), alanine aminotransferase (ALT), alkaline phosphatase (ALKP), albumin (ALB) and total bilirubin (TBIL) were measured using an IDEXX Catalyst One chemistry analyzer (IDEXX Laboratories Inc. Westbrook, ME).

Enzyme linked immunosorbent assay (ELISA)

About 35–50 mg of liver tissue stored at −80°C after euthanasia was used to extract liver protein as described previously.[73] The levels of TNFα, IL-1β, and Lcn2 were measured through ELISA according to the manufacturer's protocol (R&D Systems). The levels of hepatic TNFα, IL-1β, and Lcn2 were normalized to tissue protein content and reported as per mg tissue protein.

RNA isolation, cDNA preparation and quantitative reverse transcription polymerase chain reaction

Quantitative reverse transcription PCR (qRT-PCR) was used to evaluate hepatic gene expression related to fatty acid uptake, lipogenesis, inflammation, β-oxidation, and lipid transport. Liver tissues, preserved in RNA later (Sigma) solution, were used for total RNA extraction (Illustra RNAspin Mini, GE Healthcare). The concentration and purity of the extracted RNA was assessed using a NanoDrop spectrophotometer (Thermo Scientific). Next, RNA was converted into complementary DNA (cDNA) using the qScriptTM XLT cDNA supermix kit (QuantaBio), following the manufacturer's protocol. Specifically, 1.5 μg of RNA was reverse-transcribed. The gene expression was assessed using the QuantStudio 3 Real-Time PCR System (Applied Biosystems). Primer sequences for the target genes used in this study are provided in Table 1. Transcript levels were normalized with the housekeeping gene *36B4*, and the results are presented as 2^{-ddCT}.

Histochemical and terminal deoxynucleotidyl transferase dUTP nick end labeling (TUNEL) staining

Hematoxylin and Eosin (H&E)-stained sections along with unstained slides were prepared at the animal diagnostic laboratory, The Pennsylvania State University. H&E-stained sections were utilized to visualize the fat deposition in the liver sections. Unstained slides were used for Terminal deoxynucleotidyl transferase dUTP nick end labeling (TUNEL) staining as per manufacturer's instructions (Elabscience, USA). The imaging process was executed using a Leica DMi8 microscope, Leica Microsystems.

Quantitative assessment of hepatic lipids and hydrophilic compounds by ^{1}H NMR

In this study, ^{1}H nuclear magnetic resonance (NMR)-based analysis was employed to quantify aqueous metabolites and nonpolar lipids in the liver from both control and ethanol-fed mice, encompassing both normal TBA (nTBA) and high TBA (hTBA) groups. As previously described,[80] the three-phase extraction method with chloroform/methanol/water (2.5:2.5:2.1, v/v/v) was used to extract liver metabolites with some modifications. Specifically, approximately 50 mg of liver (wet weight) was homogenized and centrifuged, resulting in three distinct layers: an upper aqueous phase containing metabolites, an intermediate phase composed of protein and cellular debris, and a lower nonpolar lipid phase. The aqueous and lipid phases were collected into different 1.7 mL EP tubes and spin-evaporated to dryness in a SpeedVac vacuum concentrator. Dried metabolites and lipids were resuspended in 500 μL of phosphate buffer saline (0.1 M, 50% D2O, pH 7.4) containing 0.005% TSP (w/v) as internal standard and 600 μL of Chloroform-d with 0.03% TMS (v/v) as internal standard, respectively. After vortex and centrifugation, the supernatant was transferred into 5 mm NMR tubes for NMR analysis.

The proton (^{1}H) spectra were recorded at 298 K on a Bruker Avance *NEO* 600 MHz spectrometer equipped with a 5 mm TCI cryoprobe and a SampleJet sample changer. The noesygppr1d pulse sequence was utilized for the data acquisition for both aqueous metabolites and lipids with slightly different parameter sets, including spectral width, time domain data points, acquisition time, relaxation delay, mixing time, scans, and dummy scans. After acquisition, all ^{1}H NMR spectra underwent automated processing using Chenomx NMR Suite 10.0 software (Chenomx Inc. Canada), followed by manual inspection for phase, baseline, and chemical shift reference adjustments (with TSP for aqueous metabolites and TMS for lipids set at 0.00 ppm) to ensure adherence to quality standards. The aqueous metabolites were identified and quantified utilizing the in-built metabolite library and the fitting algorithm in the Chenomx software, with concentrations determined relative to the internal standard (TSP, 0.29 mM). For lipids, the binning values for each spectrum were obtained via Chenomx Profiler and the concentration was calculated for each lipid species according to the method used by Amiel et al.[80] against the known concentration of the internal standard (TMS, 0.22 mM) in excel.

Liver bile acid analysis

The examination of bile acids in liver samples involved the utilization of a Vanquish UHPLC system coupled with a TSQ Quantis Triple Quadrupole mass spectrometer (Thermo Fisher Scientific) with an ACQUITY C8 BEH UPLC column (2.1 × 100 mm, 1.7 μm) (Waters). Liver specimens (50 mg) underwent extraction using 1 mL of ice-cold methanol containing 0.5 μM deuterated internal standards, followed by homogenization step. The quantification of bile acids was accomplished through multiple reaction monitoring and selected ion monitoring modes, and the concentrations were determined via calibration using standard curves with Skyline (MacCoss Lab Software).[81]

QUANTIFICATION AND STATISTICAL ANALYSIS

Details regarding each experiment can be found in the accompanying figure legends. The normality of the data distribution was assessed using the D'Agostino-Pearson omnibus normality test. Descriptive statistics are presented as the Mean ± Standard Error of the Mean (SEM). Statistical significance between two groups was evaluated using an unpaired, two-tailed t-test. For comparisons involving more than two groups, a one-way analysis of variance (ANOVA) was initially conducted, followed by Tukey's multiple comparison tests. A significance threshold of $p < 0.05$ was applied to determine statistical significance. All statistical analyses were performed using the GraphPad Prism 10.1.2 software (GraphPad, Inc.).